1971

Analysis of burnup effect on thermal conductivity of UO2 during irradiation

Chern Hwa Tsai
Iowa State University

Analysis of burnup effect on thermal conductivity of UO_2 during irradiation

by

Chern Hwa Tsai

A Dissertation Submitted to the
Graduate Faculty in Partial Fulfillment of
The Requirements for the Degree of
DOCTOR OF PHILOSOPHY

Major Subject: Nuclear Engineering

Approved:

Signature was redacted for privacy.

In Charge of Major Work

Signature was redacted for privacy.

For the Major Department

Signature was redacted for privacy.

For the Graduate College

Iowa State University
Ames, Iowa

1971

TABLE OF CONTENTS

LIST OF SYMBOLS AND ABBREVIATIONS

A_o = interatomic distance

A_r = surface area

$\bar{a}$ = unit cell vector

a_c = absorption coefficient

b = amplitude of wave

C = specific heat

d_t = thermal diffusivity

E = energy

E_f = forbidden energy

e = electric charge

$\bar{e}_j$ = unit vector of polarization

$\bar{F}$ = electric field

f_o = equilibrium distribution function of electrons

h = Planck's constant

i = imaginary number

$\bar{i}$ = unit vector in directions of ∇T and $\bar{Q}$

$\bar{j}$ = electric current density

K = total thermal conductivity

K_e = electronic component of thermal conductivity

K_L = lattice component of thermal conductivity

K_L' = lattice thermal conductivity of pure real solid

K_r = internal radiation component of thermal conductivity

k = Boltzmann's constant

l_r = length of sample

M = atomic mass

$\bar{M}$ = mean atomic mass

N_a = Avogadro's number

N_f = number fissions/cm^3

N_n = non-equilibrium distribution function of phonons

N_o = equilibrium distribution function of phonons

n = zero or positive integers

n' = deviation of phonon distribution function

n_r = refractive index

$\bar{Q}$ = heat current density

$\dot{Q}$ = heat flow rate

$\bar{q}$ = wave vector

R = gas constant

$\bar{r}$ = space vector

S = number of lattice sites in the crystal

s = Stefan's constant

T = temperature

T_D = Debye temperature

T_m = melting point temperature

t = time

u = modulating function

V_c = crystal volume

$\bar{V}$ = mean volume

$\bar{v}$ = group velocity of wave

$\bar{v}_s$ = velocity of sound

W = watt

w_D = maximum frequency

w_j = frequency of wave component

α = thermal expansion coefficient

β = fraction of interatomic distance

γ = Gruneisen's constant

σ = electrical conductivity

λ = mean free path of phonon

ϑ = reduced energy

ψ = wave function

ρ = density

τ = relaxation time

ζ = Fermi energy

χ = compressibility

I. INTRODUCTION

Uranium dioxide exhibits a "body-centered cubic" structure and is a polycrystalline ceramic in its sintered fuel forms. One of the most undesirable properties of uranium dioxide as a nuclear fuel is its low thermal conductivity. Nevertheless, uranium dioxide is coming to be the most widely used fuel material for nuclear applications. The notable reasons for its popularity are its stability at high temperatures and neutron irradiation, and ease in manufacturing and reprocessing. Fuel cost is a major investment in a nuclear power plant; therefore, fuel performance is very important from an economic point of view as well as technological reasons such as heat transfer and neutron economy.

In general, thermal problems are relatively less critical in a low neutron flux thermal nuclear reactor than in a high flux fast reactor. In the latter, the temperature is high enough that fuel melting and swelling may occur during reactor operation. This is particularly significant when the fuel is at high burnup. Generally, when UO_2 fuel burnup increases, its thermal conductivity [35] and melting point [10] decrease. Fuel swelling is known to be a function of temperature gradient [15]. Temperature gradient, in turn

is a function of thermal conductivity. It is therefore vital to know and be able to predict the thermal conductivity of the fuel as accurately as possible in order to improve the fuel design for its better performance.

Since UO_2 is one of the semiconductors, the general theories of semiconductors are applicable to it. During the later 1950's and early 1960's, semiconductors become very important in technological application. Theoretical studies and experimental investigations on semiconductors were extensively researched. Although there are extensive data on UO_2 thermal conductivity, particularly pertaining to temperatures below 800°K, there still remains considerable disagreement among various experimental results. At high temperature ranges, the disagreement becomes more marked. As UO_2 is a compound molecule, chemical processing and sintering may not be identical for all specimens. Thermal conductivity deviation is possible for individual specimens. The difficulties in analyzing thermal conductivity experimental measurements may also be attributed to the disparity of theories. Although theories on thermal conductivity contribute to the understanding of thermal behavior of solids, their formulas generally have a wide divergence from the experimental results.

The difficulty in determining the thermal conductivity of UO_2 becomes obvious when its physical properties change as a result of increasing fuel burnup. This is particularly evident during neutron irradiation under reactor operating conditions. During irradiation, fissions constantly occur in the fuel which causes knockout of atoms, dislocation of molecules, fission product migration and ionization of fission fragments. Experimental measurements have been made on UO_2 thermal conductivity both in-pile and out-of-pile. In the Plutonium Recycle Test Reactor (PRTR) alone, 66 UO_2 fuel elements have been examined after irradiation. One of the most comprehensive reports of UO_2 thermal conductivity measurements is by Ross [35]. His application of the longitudinal heat flow method in performing out-of-pile measurements at a temperature 60°C showed that the thermal conductivity of UO_2 depends upon its density, microstructure, stoichiometry and burnup. At relatively high temperature ranges, Godfrey et al. [20] have measured UO_2 thermal conductivity up to 1100°C. Ainscough and Wheeler [1] used a modulated electron-beam method for their measurements. A 2.7% enriched UO_2 of 97% theoretical density gave the empirical formula of UO_2 thermal conductivity between 970°K and 2020°K as

$$K = (0.0227T + 3.38)^{-1} + 6.6 \times 10^{-13}T^3 \quad W/cm\text{-}^oK \quad (1)$$

For in-pile high temperature measurement, Bogaievski et al. [8] have measured UO_2 thermal conductivity up to 1200°C. In a fast reactor, temperatures higher than 1500°K are quite common in practice, although experimental data on the conductivity of UO_2 at this high temperature range are still needed.

Knowledge of the thermal conductivity of UO_2 fuel at high burnup, temperatures above 1500°K and under in-pile conditions is particularly important because it is under these conditions that higher overall operating efficiencies may be attained. Unfortunately, it is extremely difficult to make thermal conductivity measurement under such conditions. The difficulties are largely due to the factor that high temperature measurement techniques are still not highly efficient and thermocouples incorporated into the fuel may be damaged by neutron irradiation.

The purpose of this analysis is to determine the UO_2 thermal conductivity by combining theories and published experimental data to develop a semi-empirical formula for its computation at high temperature and high burnup. This is especially important where experimental measurements are difficult and idealized theoretical formulations are complicated and impractical. In this analysis, thermal con-

ductivity will be determined as a function of fuel burnup from 0.2% to 7% of theoretical density (TD) with temperatures from 773°K to 2773°K. The functional ralationship of thermal conductivity to burnup and temperature is assumed to be continuous up to the melting point of the fuel. It will be shown that the computations require rahter complicated processes. This is because the physical properties of the UO_2 fuel change at each burnup stage. These changes include density, microstructure and fission products distribution. Therefore, most of the parameters used in calculating thermal conductivity must be re-evaluated at each stage in the burnup.

II. LITERATURE REVIEW

A. Theory of Energy Transport Processes

Thermal conductivity can be described as a measure of an energy transport process in a medium from higher energy or temperature region to lower regions. Energy transport mechanisms in solid state materials are generally not well understood. Additional complications arise in a solid nuclear fuel during neutron irradiation. In general, there are three major energy transport mechanisms: (1), energy transport by phonons; (2), energy transport by electrons; and (3), energy transport by internal radiation. Among these three mechanisms, internal radiation is the least understood. Viskanta [37] has shown theoretically that for polycrystalline UO_2 the effect of internal radiation is not important. However, recent experimental results obtained by Ainscough and Wheeler [1] shown that above 1500°K, internal radiation becomes significant. Theories of energy transport by phonons and electrons have been well developed [16, 28, 40] on the basis of classical wave mechanics. The mathematics involved in determining the theoretical thermal conductivity by wave mechanics is complicated, and except for few good conductors, its accuracy is questionable. Although wave mechanics in dealing with thermal conductivity

problem is impractical, it does offer some basic understanding of the energy transport process. Therefore, it is desirable to give some background theory of energy transport process by phonon and electron waves to back up the analysis of UO_2 thermal conductivity which will be discussed in a later section. Detailed discussions, however, on the theories of energy transport process are lengthy [40]. Therefore, only important results will be given here.

1. Electron theory

In an ideal crystal, the atoms are arrayed in an orderly pattern in their lattice. The electrical potential $U(\bar{r})$ of an electron in this ideal crystal is periodic so that $U(\bar{r}) = U(\bar{r} + n\bar{a})$, where n is zero and positive integers, $\bar{a}$ is the unit cell vector. The wave function $\psi_{\bar{q}}(\bar{r})$ from the solution of the Schroedinger time-independent wave equation in such a periodic potential consists of eigenfunctions and is given [16, 28] by

$$\psi_{\bar{q}}(\bar{r}) = u_{\bar{q}}(\bar{r})\exp(i\bar{q}\cdot\bar{r}) \qquad (2)$$

where $\bar{q}$ is the wave vector, $u_{\bar{q}}(\bar{r})$ is a function has the same periodic behavior as the potential function $U(\bar{r})$. The

time dependence of the eigenfunction is expressed by

$$\psi_{\bar{q}}(\bar{r},t) = u_{\bar{q}}(\bar{r})\exp[i(\bar{q}\cdot\bar{r} - E(\bar{q})t/\hbar)] \qquad (3)$$

where i is an imaginary number in the complex plane, $E(\bar{q})$ is energy, t is time, $\hbar = h/(2\pi)$ and h is Planck's constant. Wave mechanics is basically for statistical considerations. It is the wave packet and its group velocity $\bar{v}$ which is taken into account while dealing with physical problems. The group velocity is given by

$$\bar{v} = \frac{1}{\hbar}\frac{\partial E(\bar{q})}{\partial \bar{q}} \qquad (4)$$

In a real crystal, the atoms are not perfectly arrayed in the lattice so the periodic property is disturbed. The wave functions are not actually in a stationary state as shown in Eq. (2). However, because the states involved in a wave packet are so large, a statistical equilibrium can be attained by the electron random scattering process. The electron distribution function at this equilibrium condition is

$$f_o(\bar{q}) = \frac{1}{\exp(E - \zeta)/(kT) + 1} = \frac{1}{\exp\theta + 1} \qquad (5)$$

where ζ is Fermi energy, k is Boltzmann's constant, T is temperature and θ is reduced energy as defined in Eq. (5). In terms of the equilibrium distribution function $f_o(\bar{q})$, the electric current density j and heat current density $\bar{Q}$ are given by

$$j = \left(\frac{1}{e}\frac{d\zeta}{dT}\nabla T - \bar{F}\right)\int \sigma(\theta)\frac{df_o}{d\theta}\,d\theta + \frac{k}{e}\nabla T\int \sigma(\theta)\theta\,\frac{df_o}{d\theta}\,d\theta \qquad (6)$$

$$\bar{Q} = \frac{kT}{e}\left(\frac{1}{e}\,\frac{d\zeta}{dT}\nabla T - \bar{F}\right)\int \sigma(\theta)\,\frac{df_o}{d\theta}\,d\theta + \frac{k^2T}{e^2}\nabla T\int \sigma(\theta)\theta^2\,\frac{df_o}{d\theta}\,d\theta \qquad (7)$$

where $\bar{F}$ is the electric field, e is the electric charge and σ is electrical conductivity. In the thermal conductivity problem, the electric current density is assumed to be zero, and Eq. (6) may be re-arranged to

$$\frac{1}{e}\frac{d\zeta}{dT}\nabla T - \bar{F} = -\frac{\frac{k}{e}\nabla T\int \sigma(\vartheta)\vartheta\,\frac{df_o}{d\vartheta}\,d\vartheta}{\int \sigma(\vartheta)\,\frac{df_o}{d\vartheta}\,d\vartheta} \qquad (8)$$

The thermal conductivity due to electron migration K_e is defined by

$$K_e = -Q/\nabla T \qquad (9)$$

From Eqs. (7) and (8), Eq. (9) becomes

$$K_e = \frac{k^2T}{e^2}\Big[\frac{\left(\int \sigma(\vartheta)\vartheta\,\frac{df_o}{d\vartheta}\,d\vartheta\right)^2}{\int \sigma(\vartheta)\,\frac{df_o}{d\vartheta}\,d\vartheta}$$

$$- \int \sigma(\vartheta)\vartheta^2\,\frac{df_o}{d\vartheta}\,d\vartheta\Big] \qquad (10)$$

To determine thermal conductivity of semiconductors by evaulating Eq. (10) is difficult and results are frequently inaccurate.

Experimental observations by Wiedemann and Franz based on a formula similar to Eq. (10) will be discussed in a later section.

2. Phonon theory

Energy transport by phonons may be analogous to the propagation of light wave. In an ideal crystal, an atom is bound in a position next to its neighboring atoms. At any instant, the displacement of an atom is related to the position of its neighboring atoms. If an atom undergoing a small displacement, the restoring forces are approximately proportional to the displacement. Consequently, a simple harmonic motion takes place. The motion of each atom about its mean position can be express as the superposition of a number of harmonic vibrations [16] each having its own characteristic frequency. The basis set of simple harmonic vibrations can describe all atoms in a system although the amplitude and phase of each atom varies from one to another in this system. The various simple harmonic vibrations in a particular system are defined as the normal mode. Classical quantum mechanics is applicable for such harmonic vibrations. However, the mathematics involved in a quantum mechanical treatment are complicated, and in general impractical for solving thermal conductivity problems of semiconductors. On the other hand, from a physical point of view, it has the

advantage of showing how the energy is transported in the solid by propagation of phonon waves.

The travelling phonon wave coming from vibration displacement $y(\bar{r})$ of the atom at $\bar{r}$ is expressed by [28]

$$y(\bar{r}) = \frac{1}{S^{1/2}} \sum_j \bar{e}_j b_j(\bar{q}) \exp[i(\bar{q}\cdot\bar{r} + w_j t)] \qquad (11)$$

where S is the number of lattice sites in the crystal, $\bar{e}_j$ is a unit vector describing the polarization, b_j is the amplitude of a wave identified by wave vector $\bar{q}$ and a polarization index j and w_j is the angular frequency of the wave. In quantum theory, the energy of a harmonic oscillator is not a continuous variable, but is a set of discrete values given by

$$E_j(\bar{q}) = \hbar w_j(n + 1/2) \qquad (12)$$

where n is zero or positive integers.

Since a phonon is basically energy, its motion is, therefore, an energy transport process. In a normal mode, the motion is harmonic as in an ideal crystal. The harmonic motion is a normal process or simply an N-process. In an N-process, the momentum of the phonon system is

conserved. That is, if two phonons interact, a third phonon is formed with momentum equal to the sum of those two phonons before the interaction. In this case, thermal resistance is zero or thermal conductivity is infinite.

In a real crystal, the lattice vibration is anharmonic, and momentum of the phonon system are not the same before and after interaction. The energy transport process, in this case is called the umklapp process or simply U-process [26] after German for "flipping over". The loss of momentum or energy during this process is due to the existing thermal resistance in the solid. It is the U-process that dominates the theory of lattice thermal conductivity.

Each lattice mode of wave has an energy kT. The Boltzmann distribution function in statistical thermal equilibrium gives the average number of phonons in a mode of frequency w as

$$N_o = \frac{1}{\exp(\hbar w/kT) - 1} \qquad (13)$$

In dealing with non-equilibrium situations, the energy interchange mechanism approaching equilibrium is of main concern. The rate at which a non-equilibrium distribution

will tend to become equilibrium by thermal conduction is governed by the relaxation time. If N_n is the non-equilibrium distribution function of phonons, the time rate of change N_n, and the gradient N_n, in turn, are functions of temperature gradient, this gives the relationship by which

$$\left.\frac{dN_n}{dt}\right|_{\nabla T} = - \bar{v} \cdot \text{grad } N_n = - (\bar{v} \cdot \text{grad } T) \frac{dN_o}{dT} \qquad (14)$$

If $n'(\bar{q})$ is the phonon distribution deviation from the equilibrium distribution of N_o due to anharmonic processes by phonon interactions, then the non-equilibrium distribution is $N_n = N_o + n'$, so the time rate of change of N_n is

$$\left.\frac{dN_n}{dt}\right|_{int} = - \frac{n'(\bar{q})}{\tau(\bar{q})} \qquad (15)$$

where $\tau(\bar{q})$ is relaxation time. At a steady state, $dN_n/dt = 0$, the right hand side of Eqs. (14) and (15) are equal, hence,

$$n'(\bar{q}) = - (\bar{v} \cdot T)\, \tau(\bar{q}) \frac{dN_o}{dT} \qquad (16)$$

The velocity $\bar{v}(\bar{q})$ is the group velocity of the phonon wave

packet, and is expressed by

$$\bar{v}(\bar{q}) = \frac{dw_j(\bar{q})}{d\bar{q}} \tag{17}$$

The heat current is given by

$$\bar{Q} = \sum_{\bar{q},j} \bar{v}\hbar w_j N_n(\bar{q}) \tag{18}$$

In equilibrium, $\bar{Q} = 0$, the states of $\bar{q}$ and $-\bar{q}$ of opposite velocity but equal energy can be offset. Thus it can be assumed $N_n(\bar{q}) = n'(\bar{q})$ and Eq. (18) becomes

$$\bar{Q} = \sum_{\bar{q},j} \bar{v}\hbar w_j n'(\bar{q}) \tag{19}$$

From Eqs. (16) and (19), the thermal conductivity K_L' by phonons can be expressed by

$$K_L' = -\frac{\bar{Q}}{\nabla T} = \sum_{\bar{q}} (\bar{v}\cdot\bar{i})^2 \tau(\bar{q}) C(\bar{q}) \tag{20}$$

where $\bar{i}$ is a unit vector in the direction of ∇T and $\bar{Q}$ respectively, and $C(\bar{q}) = \hbar w_j dN_o/dT$ is specific heat. If the mean free path of the phonon is $\lambda(\bar{q}) = v\tau(\bar{q})$, Eq. (20) would take the form of Debye's formula of thermal conduc-

tivity which will be given in Section III. Eq. (20) is a general equation for real solids due to anharmonicity from not idealized lattice geometry. The relaxation time is very difficult to determine even approximately, so Eq. (20) is not generally used directly.

As mentioned earlier, the thermal conductivity of UO_2 is very complicated due to neutron irradiation which leads to fission products concentration, molecules dislocation, etc. There have been several studies made on thermal conductivity of imperfection(with impurities) solids. Morgan [34] has done an extensive theoretical analysis on the thermal conductivity of structurally disordered solids based on Eq. (11). Klemens [27] and Ambegaokar [2] have done a theoretical analysis of thermal resistance due to point defects at high temperatures. These analysis will be partially applied to handle this problem later.

B. Methods of Thermal Conductivity Measurement

Although the thermal conductivity of UO_2 considered in this study will be analyzed analytically, the basic principles of experimental thermal conductivity measurements and techniques applied to UO_2 fuel will be also outlined.

The general equation for thermal conductivity is given by

$$K = \frac{\dot{Q}}{A_r \nabla T} \qquad (21)$$

where $\dot{Q}$ is the heat flow rate, A_r is area of the measuring sample and T is temperature gradient.

The greatest difficulty in measuring thermal conductivity is in preventing radiation heat loss. Heat Radiation is a direct function of the fourth power of temperatures. At high temperatures, the accuracy of the measurement becomes more difficult. The temperature gradient in Eq. (21) is determined by measuring temperatures in the direction perpendicular to A_r.

Basically, there are two methods of measurement, the steady state(static) and the transient(dynamic) methods. These methods have been used since the 19th century. There are approximately 800 references on thermal conductivity measurements listed on the data books of the Thermophysical Properties Research Center [29]. The accuracy of measurement may not be attributed to the methods applied but rather to the details of the actual experimental techniques. The quantity of thermal conductivity can not be measured directly as shown in Eq. (21), but the actual

measurable quantity is temperature gradient or temperatures. At temperatures above room temperature, thermocouples are generally used for temperature measurements.

Although other means of supplying a heat source may be used, electrical heating is the most convenient and widely used.

1. Static heat flow measurement

In static heat flow measurements, after heat energy is supplied to the sample, temperature measurement is taken only after thermal equilibrium is reached. The main disadvantage of this method is the long waiting time required before temperature measurements can be taken. The advantage of this method is its relative ease in obtaining accurate measurements. The static method may be done with direct measurements or comparative techniques.

a. Direct measurement Due to radiation heat loss, direct measurements may be applied for samples at room temperature or below. However, at higher temperatures the results become less accurate. In an axial heat flow direct measurement, the heat loss may be reduced by using short samples or larger contact surface samples. The shortcoming of a short sample is the difficulty in obtaining accurate

temperature gradient. In general, test samples of UO_2 fuels have a small contact surfaces. An apparatus for direct measurement employed by Goldsmid [16, 21] is shown in Fig. 1.

b. Comparison measurement At high temperatures, radiation heat losses by the test sample become high. In this case, if the measurement is to be made by axial heat flow, the comparison measurement is preferred. The procedure of the comparison measurement is to use standard samples of known thermal conductivity, and preferably with similar physical properties, as the test sample. The test sample is sandwiched between two standard samples. Of these standard samples, only temperatures need be measured in order to determine the heat flow rate $\dot{Q}$ by Eq. (21).

The comparison technique has been employed by A. M. Ross [35] is measuring the thermal conductivity of UO_2. An axial heat flow apparatus constructed by Ross for his measurement is shown in Fig. 2.

2. Dynamic method

In the so-called dynamic method, after heat is supplied, the temperature measurements are made before the equilibrium condition is attained. In such a system, the time required for each observation of temperatures in an experiment is

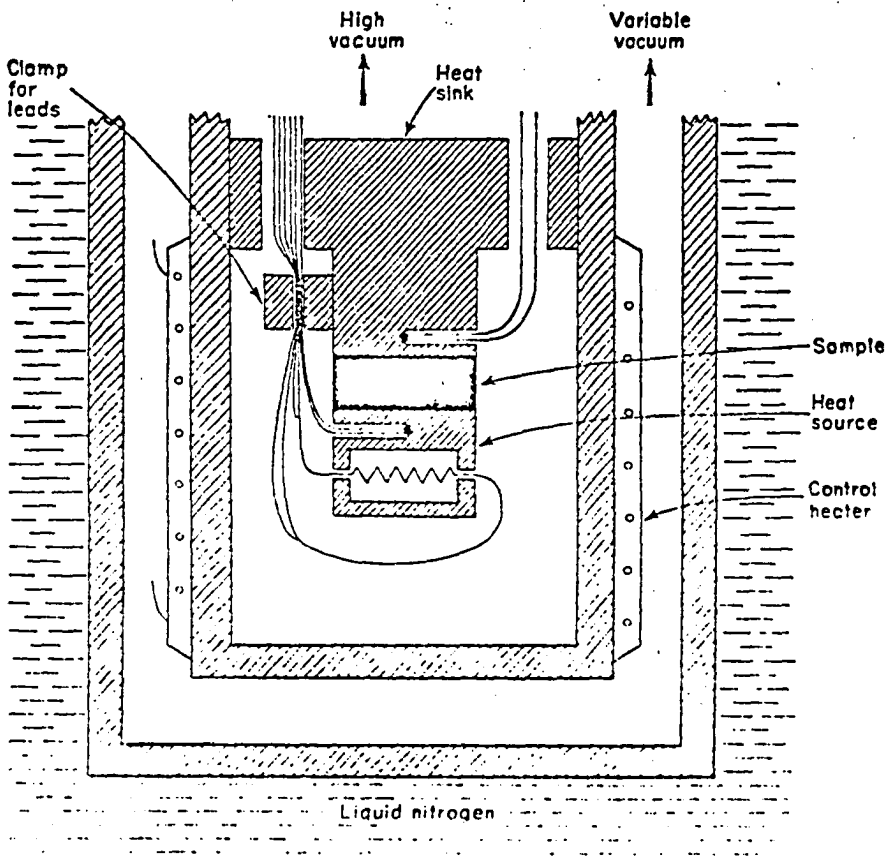

Fig. 1. Goldsmid's apparatus for thermal conductivity measurement.[16, 21].

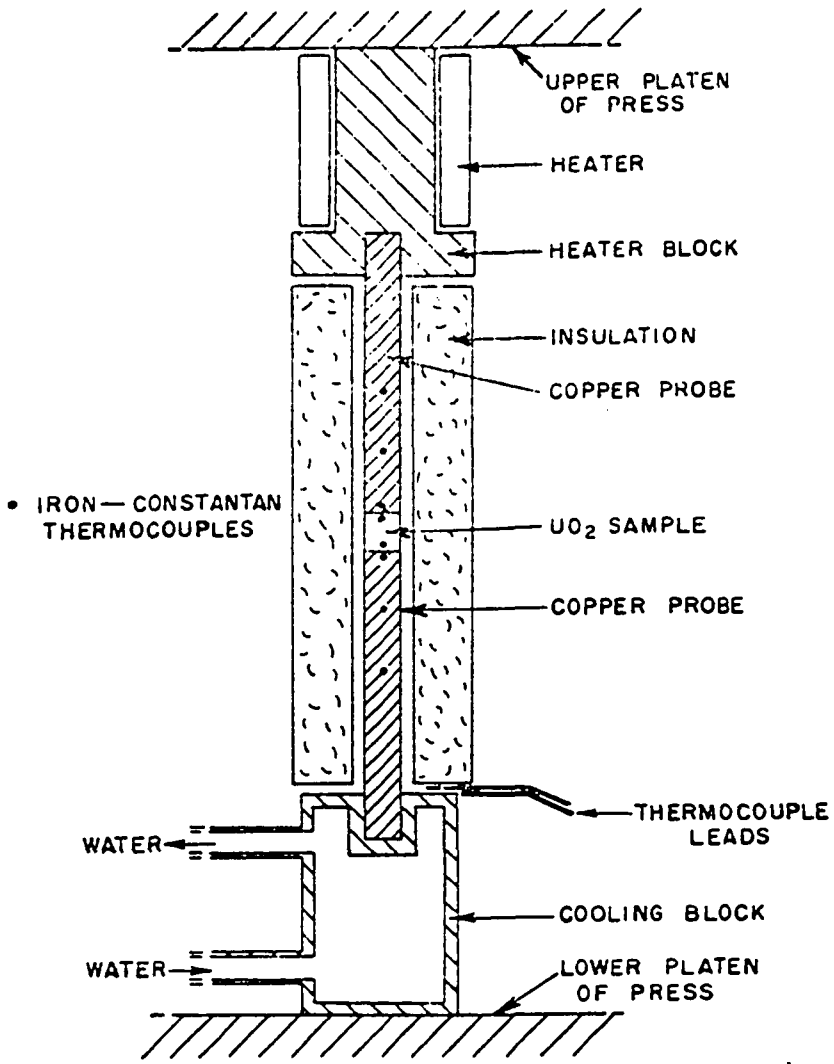

Fig. 2. Ross's apparatus for UO_2 thermal conductivity measurement. [35].

greatly minimized. Although a large number of experiments have been performed by different experimenters, for simplicity the apparatus of Ioffe and Ioffe is shown in Fig. 3.

The examples discussed employed an axial heat flow technique for temperature measurements. Often radial heat flow also employed in UO_2 nuclear fuel has cylindrical geometry. The burnup may vary in the radial direction and it seems that radial heat flow measurements may be suitable in this case. The radial heat flow measurement has been discussed in detail by McElroy and Moore [32].

3. Periodic heat flow measurement

This method is employed to determine thermal diffusivity directly by supplying heat source periodically through the test sample. Angstrom [3, 16] developed this method in 1861, and a number of experimenters have employed this method for thermal diffusivity measurements. One of the most detailed discussion on such measurement were made by Danielson and Sidle [12]. If the specific heat and density ρ of the solid are known, thermal conductivity K can be derived indirectly from the known thermal diffusivity d_t by

$$K = d_t C \rho \qquad (22)$$

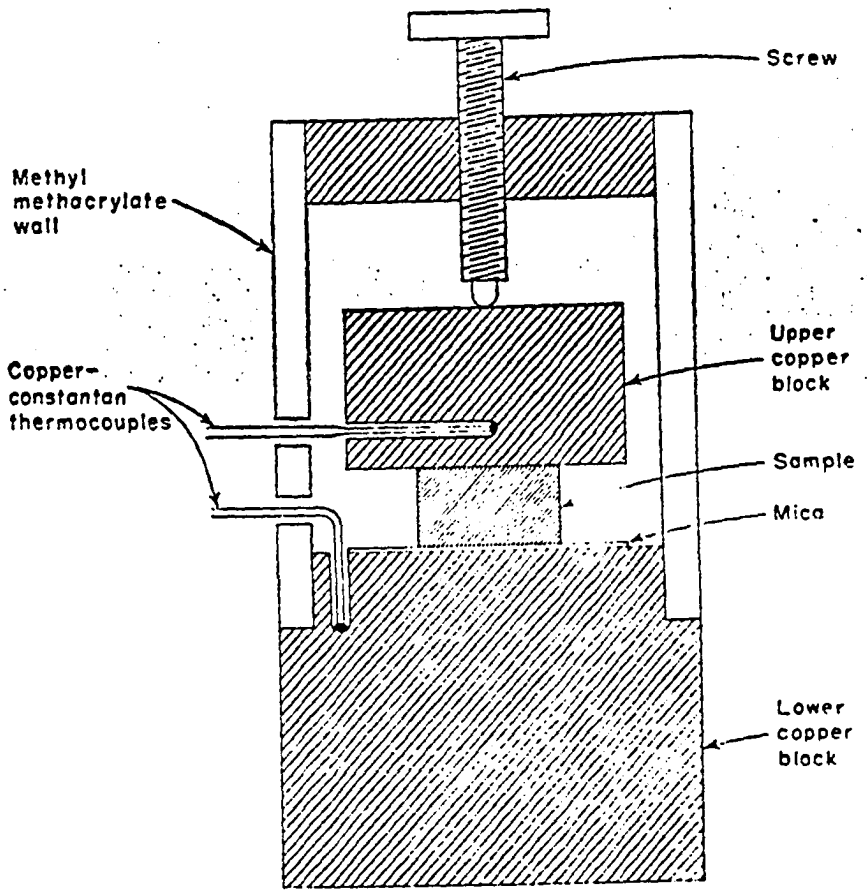

Fig. 3. Ioffe and Ioffe's apparatus for thermal conductivity measurement [16, 23].

4. Fuel capsule for in-pile measurement

The experimental techniques discussed and illustrated are for measuring thermal conductivity of solid in general, but can not be used for in-pile measurement of nuclear fuel during neutron irradiation. For this kind of measurements it may be desirable to design a special fuel capsule containing the test sample with positioned thermocouples. One such capsule is shown in Fig. 4 [11].

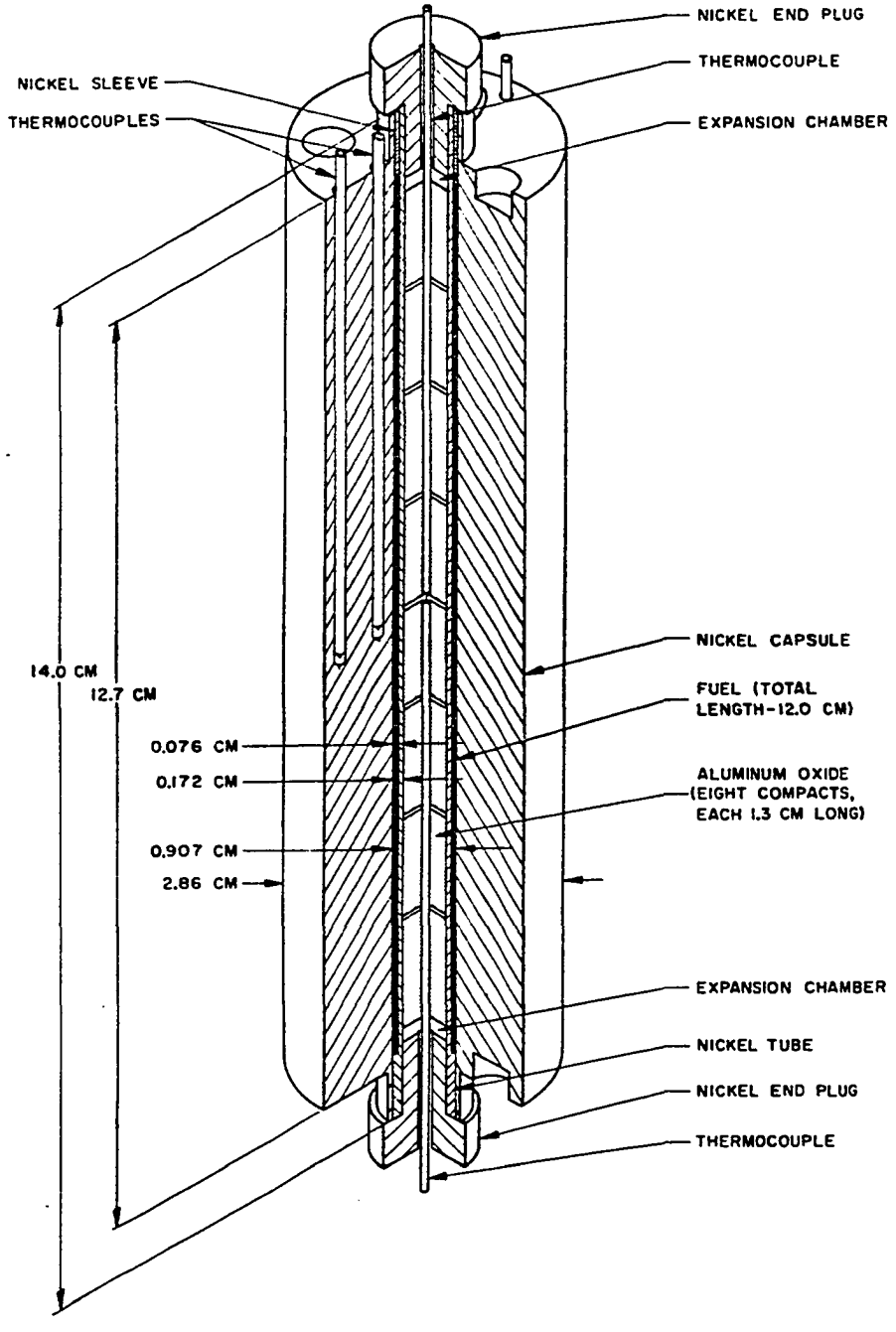

Fig. 4. UO_2 fuel capsule for thermal conductivity measurement [11].

III. ANALYSIS OF UO_2 THERMAL CONDUCTIVITY

A. Fuel model and Method of Analysis

The original fuel is assumed to be freshly sintered homogeneously stoichiometric UO_2 in a cylindrical geometry with theoretical density(TD) of 10.95 gm/cm^3. After some burnup has occurred, the partially depleted fuel is considered to have oxygen excess, and non-stoichiometric UO_2 is assumed. Neutron flux in the fuel is a function of radius r, and is independent of azimuth angles. Thus, the rate of fission is isotropic, and hence no heat flow occurs in the the azimuth direction. This assumption may be supported by Fig. 5 where a cross-section of a used fuel element shows the seam of the fractures uniformly along the radial direction. The reactor is assumed in continuous operation and whenever the power level changes it is taken slowly so that the fission products distribution has a predictable pattern.

The method of analysis presented here is a combination of theoretical formulations and experimental results to form a semi-empirical basis for computations. Coefficients and parameters needed for calculation will be adopted from published values, extrapolation of experimental data and conservatively estimated.

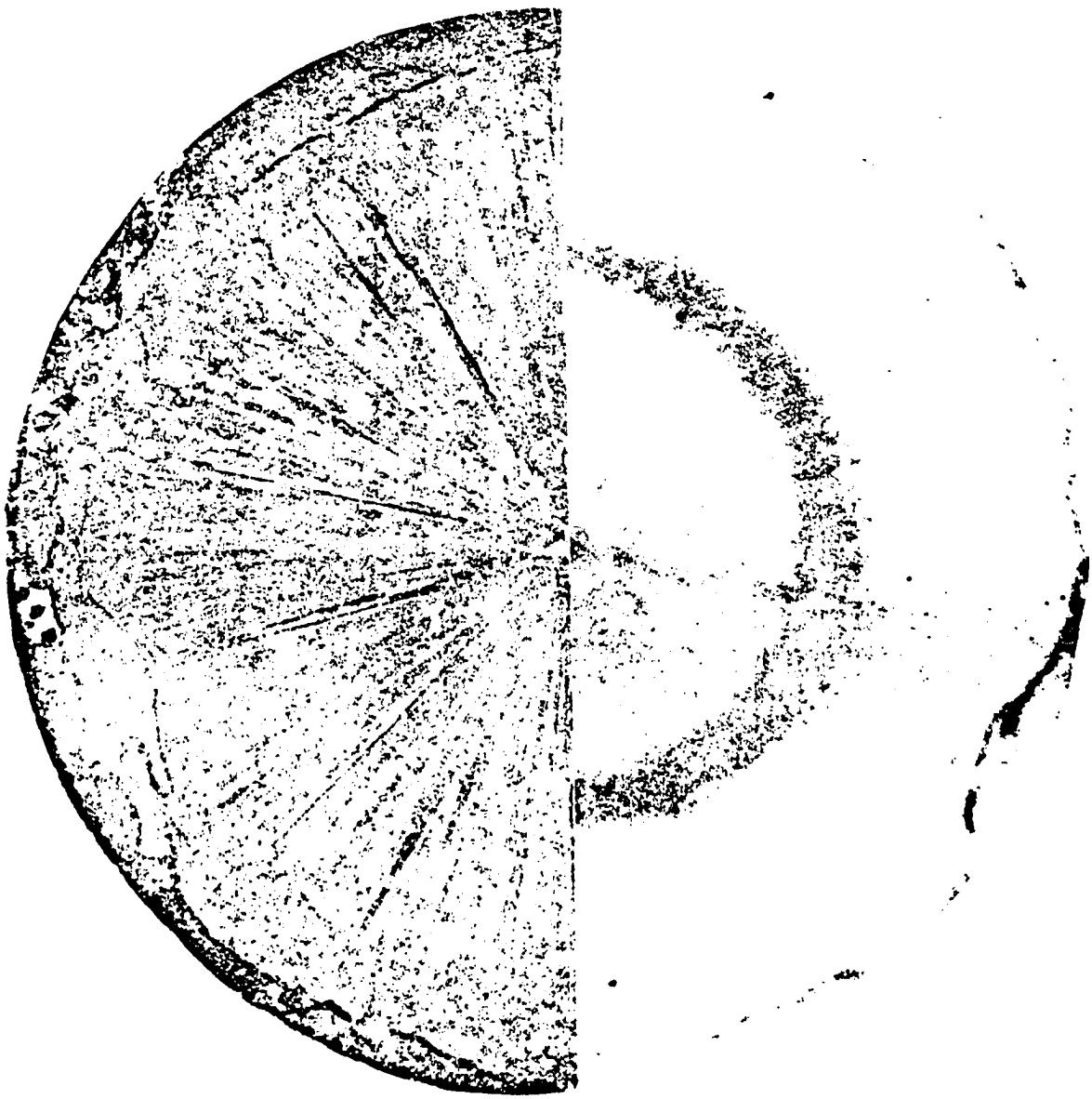

Fig. 5. Irradiated UO_2 fuel cross-section (4.7×10^{20} fissions/cm^3) [5].

The total thermal conductivity K will be calculated by the sum of electronic component of thermal conductivity K_e, lattice component of thermal conductivity K_L and internal radiation component of thermal conductivity K_r in the form

$$K = K_e + K_L + K_r \qquad (23)$$

The calculations will be performed at various temperature intervals from 773°K to 2773°K. Each temperature interval corresponds to the neutron flux or power level of the reactor. In this way the burnup rate is approximately constant. At each temperature interval, the thermal conductivity is determined at various burnup stages.

B. Fission Product Concentration

The fresh non-irradiated UO_2 fuel is assumed to be homogeneous. In an irradiated UO_2 fuel, due to fission product migration, the homogeneous assumption is no longer applicable. As it can be seen in Fig. 5, there is an annular region where the fission product concentration is much higher. However, Fig. 5 is an out-of-pile irradiated fuel cross-section. The in-pile fission product distribution during irradiation may not be the same. The characteristic of fis-

sion product distribution is not unique, it varies from fuel element to fuel element, and depends upon the level of neutron flux irradiation [6]. It might be also influenced by the frequency of power level changes which includes reactor shut down and re-start up. From theory as well as shown in Fig. 5, it is evident that the concentration varies along the radial direction only. This suggests that the thermal conductivity of the irradiated UO_2 fuel has a radial dependence.

The fission product gases of xenon and krypton constitute about 12% of the fission products. Their migration down the thermal gradient may have a positive contribution to the energy transport processes. However, because of the limited quantity of these fission gases, the maximum amount of heat transfer by gases can be demonstrated to be not more than 0.1% of the heat transfer by the solid portion of the fuel.

C. Electronic Component of Thermal Conductivity

The theoretical derivation of the electronic component of thermal conductivity K_e has showed in Eq. (10). On the basis of experimental observation for metals, Wiedemann and Franz gave the expression of electronic component of thermal conductivity as

$$K_e = 2 \frac{k^2}{e^2} \sigma T \qquad (24)$$

which is the well known Wiedemann-Franz law. It stated that the ratio of the thermal conductivity to the electrical conductivity is a constant for all metals at a given temperature. For semiconductors, the Wiedemann-Franz law is generally applicable. For extrinsic semiconductors Eq. (24) is satisfied. For intrinsic semiconductors the relationship is given [16] by

$$K_e = \frac{\pi^2}{3} \frac{k^2}{e^2} \sigma T \qquad (25)$$

It is the Wiedemann-Franz law that this analysis will be based upon for its calculation in determining the electronic component of thermal conductivity. From Eqs. (24) and (25), it is seen that K_e is directly proportional to the electrical conductivity. Its measurement is required in order to determine K_e for any given temperature. Therefore, the electrical conductivity of UO_2 as it changes at various burnup stages needs to be determined. A semiconductor in a relatively low temperature range has the properties of P-type or N-type with difference in electrical conductivities [38]. In a higher temperature range, the tightly bound

electrons may have enough energy to free themselves from the atom, and the semiconductor changes from an extrinsic to an intrinsic semiconductor. However, its electrical conductivity is not affected by the behaviors of P-type or N-type. In a fission reactor, the temperature is high, and the charged particles produced are numerous in addition to the increase in impurities from fission products in the solid resulting in strengthening of its intrinsic behavior.

The extrinsic and intrinsic properties of a semiconductor may be best described by their energy bands [26] as illustrated in Fig. 6. to insure the theory further, it is assumed that at absolute zero temperature a vacant conduction band is separated by a forbidden band with energy E_f from a filled valence band. As the temperature is increased, electrons receiving energy greater than E_f may move up to the conduction band leaving holes in the valence band. These higher energy electrons in the conduction band and the newly created hole in the valence band contribute to the electrical conductivity increase in a semiconductor.

In addition, two other mechanisms may contribute to the increment of electrical conductivity in an UO_2 fuel during neutron irradiation. There are the impurities and ionization of fission fragments in the fuel. Assuming the

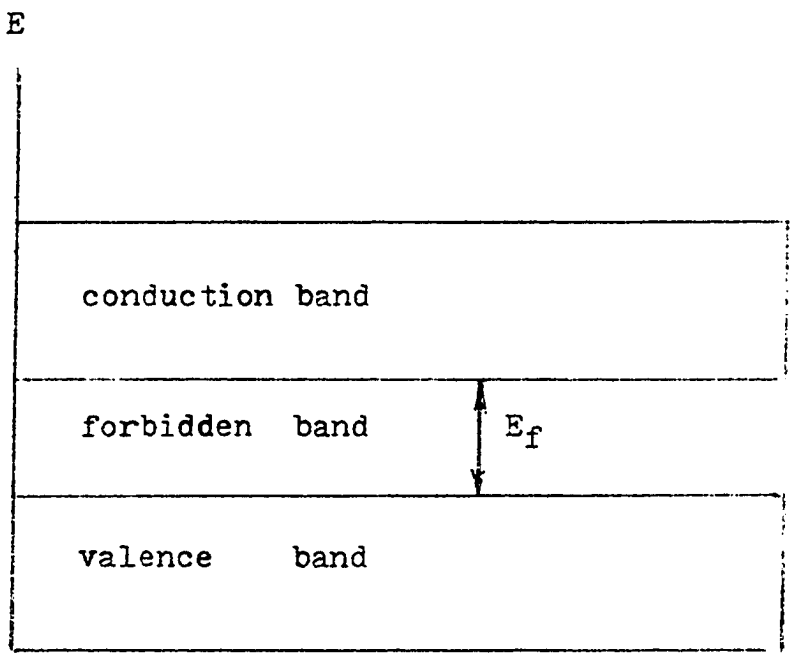

Fig. 6. Energy band of cemiconductor.

ion pairs produced by fission fragments are neutralized when the fission fragments are stopped by the solid, the amount of ionization involved contributes little to the electrical conductivity. At a constant temperature, the electrical behavior of UO_2 during irradiation can be considered effected by impurities only.

The impurities in a burnup UO_2 fuel are the fission products of uranium and oxygen of the UO_2 molecule. The plutonium produced is assumed negligible. Statistically, for each fissioned UO_2 molecule, approximately half of its remaining oxygens are oxided with its fission products [18]. The changes of electrical conductivity of a semiconductor by impurities is a result of changed covalent bonds of the molecules [36]. The principal fission products as shown in Table II do not share their valences with the UO_2 molecules. However, some of the elements are oxided with excess oxygens from fissioned UO_2. Therefore, those fission products share their valences among themselves. Oxided fission products have electrical conductivity comparable to that of UO_2. One of the oxided fission products MoO_3 is believed to have a negative effect on UO_2 electrical conductivity. It has been observed [39] that a UO_2 sample containing MoO_3 has decreased electrical conductivity above 500°C. Fission product metal may have higher electrical conductivity

than their oxides, but it only about 18%. These metals are scattered among the low electrical conductivity oxidized molecules and hence have no significant conductivity. Therefore, for each UO_2 fissioned, it is assumed the equivalent of three oxygens are produced. Since the excess oxygen has a higher doping effect than fission products as discussed, the assumption of "three equivalent oxygens" may have over estimated the electrical conductivity of the irradiated UO_2 fuel, but it will be shown later that the electronic component of thermal conductivity is still insignificant. The higher oxidation will certainly take place in the fuel due to oxygen excess, and this effect is assumed to be included in the case of oxygen excess.

The stoichiometric UO_2 is an extrinsic semiconductor under 1400°K [7]. It has been shown by Moore and McElroy [33] that at 1400°K, the electronic component of thermal conductivity of stoichiometric UO_2 is only 0.02% of its total thermal conductivity and is therefore negligible.

Ishii et al.[24] have shown experimentally that the electrical conductivity is very sensitive to the hyperstoichiometric UO_{2+x}, where x is the increase with excess oxygen of fissioned UO_2 molecules. For $x = 0.01$

at temperature 770°K, electrical conductivity increased remarkably to about 100 times higher than the stoichiometric UO_2 at the same temperature [24].

In calculating the electronic component of thermal conductivity, Eq. (24) will be used for stoichiometric UO_2 at temperature up to 1400°K. Eq. (25) will be used for stoichiometric UO_2 above 1400°K and hyperstoichiometric UO_{2+x} at all desired temperatures. The electrical conductivity will be determined from the experiment data of Ishii et al. as shown in Fig. 7 which is given for temperatures up to 1873°K. Above this temperature, the functional relationship of electrical conductivity and the fractional value x will be extrapolated from Ishii et al.'s data.

As the burnup increase, the density of the UO_2 fuel proportionately decreases. Correction must be made on the electrical conductivity due to porosity of the fuel with the correction formula given [24] by

$$\sigma = \left(1 + \frac{P}{1 - P^{2/3}} \right) \sigma_o \qquad (26)$$

where P is the volume fraction of the UO_2 specimen, and σ_o is the electrical conductivity of a standard specimen with known density. The various values of x will be

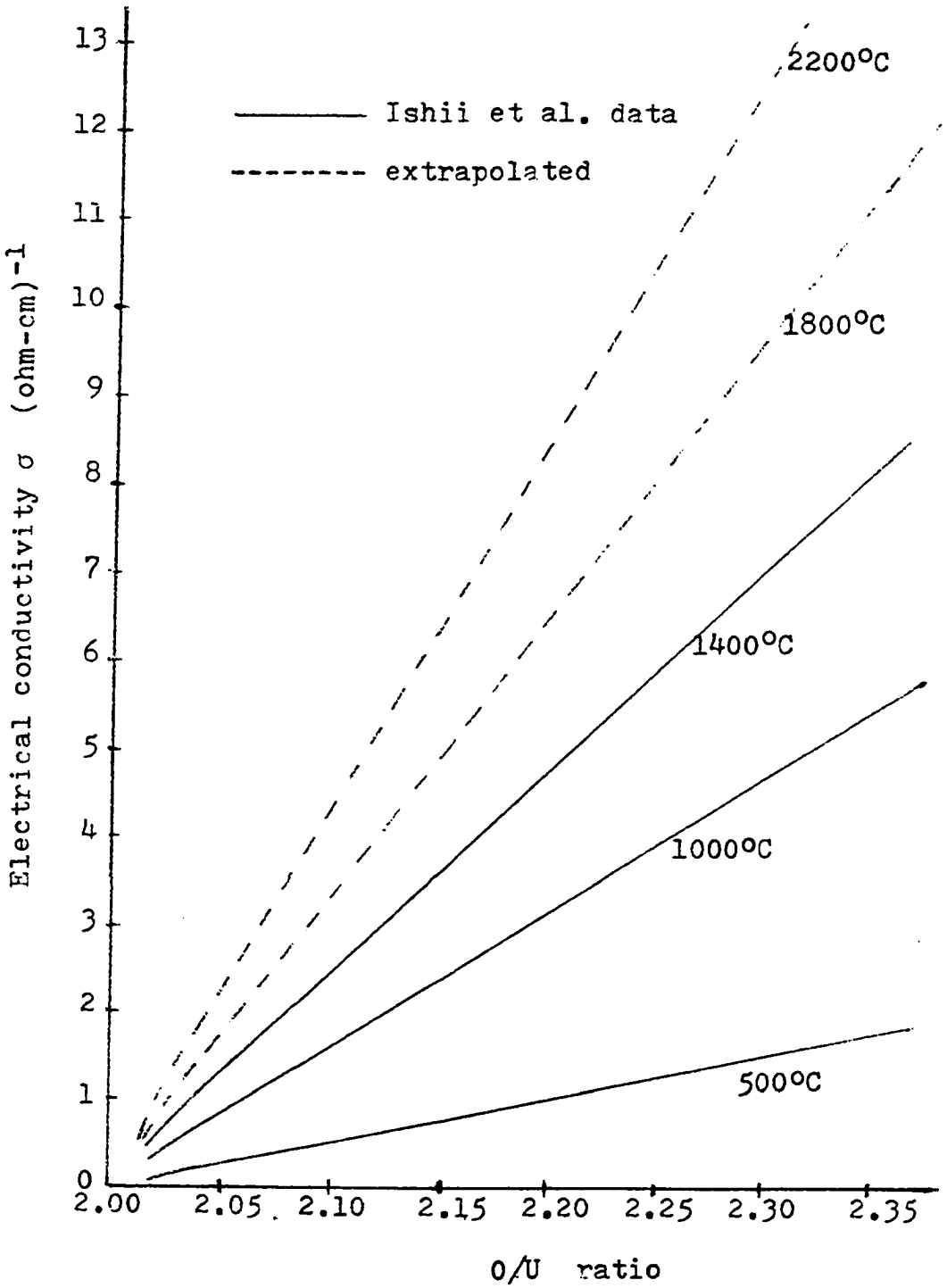

Fig. 7. Electrical conductivity of non-stoichiometric UO_2.

determined from burnup depletion at various intervals and will account for three oxygens produced per each UO_2 fission.

D. Internal Radiation Component of Thermal Conductivity

The energy radiation is known to be directly proportional to the fourth power of temperatures. Below 1500°K, the internal radiation contribution to thermal conductivity is negligible [1], but becomes more significant at higher temperatures. de Halas [14] has theorized "that the radiation heat transfer in UO_2 increases less rapidly than third power of temperatures. As the concentration of fission products in the UO_2 lattice increased, its opacity also increases and the internal radiation would decrease." Because the fission product concentration may have a polarization effect on the originally neatly arrayed UO_2 molecules in their lattice, the de Halas theory in this regard seems to be reasonable. However, opposite but not contradictory to the de Halas theory is that the fuel burnup increases, diffusion of fission gases and migration of solid fission products would increase the porosity of the fuel which would in turn increase the radiation component of heat transfer. As can be seen in Fig. 5, the vacancies created by the fractures in the fuel after irradiation would have better

radiation heat transfer. The dark annular region in Fig. 5 is higher in fission product concentration where the opacity may be higher. However, since 16% of the fission products are metals, this will increase the over all heat transfer in the dark annular region since the metals are better conductors. Therefore, the effect of the increased opacity by fission products is small compared to its positive effects increasing heat transfer.

Genzel [19] has shown that the internal radiation component of thermal conductivity K_r is proportional to third power of temperature.. His formula has been widely cited in the literature in the form

$$K_r = \frac{16\, n_r^2\, s\, T^3}{3a_c} \qquad (27)$$

where n_r is the refractive index, s is Stefan's constant of radiation and a_c is the absorption coefficient. Eq. (27) has been proved in good agreement with experimental results on a semiconductor such as tellurium [16]. The numerical values of parameter n_r and a_c for UO_2 are [1]

$$n_r = 2.2$$

$$a_c = 300 \text{ cm}^{-1}$$

The value os s is 5.67×10^{-12} joules/cm^2-sec-deg^4.

E. Lattice Component of Thermal Conductivity

In Section II, the thermal conductivity derived by phonon wave theory was expressed in the basic Eq. (20). In this section, the equations for calculating the lattice component of thermal conductivity under various conditions will be given.

1. Thermal conductivity of pure real solid

The pure real solid is defined here as a solid in its natural state containing structural imperfections but without impurities. To derive the thermal conductivity of the real solid K_L' based on kinetic theory of gases, Debye [13] treated the thermal resistance as the result of phonon scattering and applied an analogy between such scattering and diffusion or thermal conduction in gases. Thus the lattice component of thermal conductivity is given in the form

$$K_L' = \frac{1}{3} C \bar{v}_s \lambda \qquad (28)$$

where $\bar{v}_s$ is the average phonon velocity. Debye assumed that the phonon velocity is equal to the velocity of sound, and λ is the mean free path of the phonon. It is seen that Eq. (28) has the form of Eq. (20) as mentioned earier.

The mean free path λ is difficult to determine accurately. Dugdale and MacDonald [17] suggested that the mean free path λ may be empirically taken as

$$\lambda = \frac{A_o}{\alpha\gamma T} \tag{29}$$

where A_o is interatomic distance, α is thermal expansion coefficient and γ is Gruneisen's constant. Lawson [30] related the density ρ and $\bar{v}_s$ to the isothermal compressibility χ by

$$\frac{1}{\chi} = \bar{v}_s^2 \rho / g \tag{30}$$

where g is gravity. Combined Eqs. (28) to (30) and using Gruneisen relation $\gamma = \alpha/C\chi$ and give

$$K_L' = \frac{g^{1/2} A_o}{3T\gamma^2 \chi^{3/2} \rho^{1/2}} \tag{31}$$

Keyes [25] applied the Lindemann melting rule [31] which assumed that the amplitude of the thermal vibrations of the atoms reaches some fraction β of the interatomic distance at melting point temperature, and β is constant for all materials. Keyes eliminated χ by letting

$$\gamma = \frac{\beta^2 V}{R T_m} \qquad (32)$$

where V is volume per mole of atoms, R is gas constant and T_m is melting point temperature. To modify Eq. (31) further to a more familiar form, letting the interatomic distance $A_o = (V/N_a)^{1/3}$, and $V = M/\rho$, where M is the atomic weight and N_a is Avogadro's number and substituting Eq. (32) into Eq. (31), Keyes arrived at the formula for the lattice component of thermal conductivity of a pure real solid

$$K_L^{\bullet} = B \frac{T_m^{3/2} \rho^{2/3}}{M^{7/6} T} \qquad (33)$$

where

$$B = \frac{g^{1/2} R^{3/2}}{3\gamma^2 \beta^3 N_a^{1/3}} \qquad (34)$$

Keyes simplified Eq. (33) by assuming B to be constant for all materials with the value $B = 1/30$. However, experimental data has shown that B differs from material to material. Nevertheless, if B is known for a particular

material, Eq. (33) is a very useful semi-empirical formula. If the lattice component of thermal conductivity of a material is known experimentally, B can be determined from Eq. (33) as

$$B = \frac{K_L' \, T \, M^{7/6}}{T_m^{3/2} \, \rho^{2/3}} \qquad (35)$$

Keyes has applied this method to determine B for several materials. The parameter B for UO_2 will be determined later from Eq. (35).

2. Thermal conductivity of an imperfect solid

In this analysis, it is at the high temperature range that the thermal conductivity of UO_2 is of primary interest. The thermal resistance due to imperfection solids at high temperatures have been worked out by Ambegaokar [2] and Klemens [27] by relaxation time method. On the basis of their works, Drabble and Goldsmid [16] give the lattice component of thermal conductivity K_L of an imperfect solid in the form

$$K_L = K_L'(w_o/w_D)\tan^{-1}(w_D/w_o) \qquad (36)$$

and give

$$\frac{w_o^2}{w_D^2} = \frac{1}{2\pi^2 \bar{v}_s K_L' w_D A'} \tag{37}$$

where w_D is maximum frequency of phonon wave on the basis of Debye model, w_o is some frequency defined $\tau(w_o) = \tau'(w_o)$ where τ and τ' are the relaxation times of imperfection and pure real solids. The parameter A' is defined as

$$A' = \frac{\Sigma\, x_i (M_i - \bar{M})^2}{4\pi \bar{v}_s^3 N_v \bar{M}^2} \tag{38}$$

where x_i is the fraction of impurity atoms of mass M_i, N_v is the number of atoms per unit volume and $\bar{M} = \Sigma\, x_i M_i$ is the mean mass per atom. The maximum angular frequency w_D may be given [16] by

$$w_D = kT_D/h \tag{39}$$

There are two mechanisms by which impurities affect the thermal conductivity: one is by scattering phonons due to the density change locally, and the other is by altering the interatomic force strengths due to the impurity introduced local variations in the elastic properties. It is obvious that the effects of the latter are more important

in the burnup UO_2 system. In general, in a single isotope, the effects of the latter are negligible, and the term w_D/w_o is small. For an alloy or compound such as UO_2 the term $\tan^{-1}(w_D/w_o)$ is more important.

It is important here to clarify the thermal conductivity of the pure real solid K_L^* and thermal conductivity of the imperfection solid K_L. In UO_2 nuclear fuel, K_L^* and K_L are defined as its non-irradiated and irradiated thermal conductivity respectively. However, it is important to re-define or emphasize the characteristics of K_L^* which is also defined as thermal conductivity of the unirradiated portion of an irradiated UO_2 fuel. For a particular fuel element, other differences between an "irradiated portion" and a non-irradiated UO_2 are their density and melting point temperature. Since K_L is a function of K_L^* in Eq. (36), its definition is clear.

The Debye temperature, T_D, and the velocity of sound, $\bar{v}_s$, shown in Eqs. (37) and (39) are difficult to determine accurately. There are numerous data giving the value of T_D with wide range of difference from 154°K to 870°K. Theoretically T_D may be estimated [16] from the Lindemann melting rule

$$T_D = \frac{H T_m^{1/2} \rho^{1/3}}{\bar{M}^{5/6}} \tag{40}$$

where H is a constant given as $H = 120$. By the Debye approximation, the velocity of sound in terms of T_D is given by

$$\bar{v}_s = \frac{T_D k (4\pi \bar{V}/3)^{1/3}}{h} \tag{41}$$

where $\bar{V}$ is mean volume per molecule. The uncertainties of T_D and $\bar{v}_s$ is the disadvantage aspect of the theory. Nevertheless, T_D and $\bar{v}_s$ have their physical significance in the formulation of thermal conductivity and can not be ignored. In order to solve this dilemma, the constant H may be assumed unknown and it may be determined empirically from experimental data. By combining Eqs. (36) to (41), K_L for a compound substance such as UO_2 may be written in the form

$$K_L = \left(\frac{1}{1.32 \times 10^{13}} \frac{K_L' \bar{V}^{2/3} N_v H T_m^{1/2} \rho^{1/3}}{A'' \bar{M}^{5/6}} \right)^{1/2} \cdot \tag{42}$$

$$\cdot \tan^{-1}\left(1.32 \times 10^{13} \frac{K_L' A'' \bar{M}^{-5/6}}{\bar{V}^{2/3} N_v H T_m^{1/2} \rho^{1/3}}\right)^{1/2}$$

where

$$A'' = \sum_i x_i (M_i - \bar{M})^2 / \bar{M}^2 \qquad (43)$$

3. The parameter B

To determine the parameter B, Eq. (35) may be used

$$B = \frac{K_L' T \, M^{7/6}}{T_m^{3/2} \rho^{2/3}}$$

In a non-irradiated UO_2 fuel, T_m and M are constants, thus they can be calculated from the known properties. B will be a constant if the product of $K_L'T$ is a constant. In general, K_L' can not measured directly by experimental procedures and is deduced from the total thermal conductivity K of a non-irradiated UO_2 fuel by

$$K_L' = K - K_e - K_r \qquad (44)$$

where K_e can be calculated by Eq. (24) or (25) and K_r by Eq. (26). The values of total thermal conductivity K of non-irradiated UO_2 have been obtained by numerous experimenters, one of the most recent data on K is obtained experimentally by Asamoto et al. [4] as shown in

TABLE I

Thermal Conductivity of Non-irradiated UO_2 (93.4% T.D.)[4]

$T^{o}K$	K W/cm-^{o}K	TK
773	0.0425	328
873	0.0376	328
973	0.0341	331
1073	0.0314	337
1173	0.0294	345
1273	0.0278	354
1373	0.0264	363
1473	0.0253	374

Table I. The products of KT in Table I are approximately constant below 1000°K and increasing above 1000°K. This indicated that above 1000°K the internal radiation component is beginning to arise significantly, and below 1000°K the value of K is contributed by the lattice component only. Hence $K = K_L$ below 1000°K. Since Table I was obtained from data on non-irradiated UO_2, $K_L = K_L'$ below 1000°K. The product of KT below 1000°K is approximately 328, this value can be substituted into Eq. (35) to determine B. The value of B determined from the experimental data of Asamoto et al. is B = 0.0292 for non-irradiated UO_2 fuel, which is surprisingly close to the value B = 1/30 for all materials assumed by Keyes.

4. The melting point temperature T_m

One of the limitations on UO_2 fuel is its decrease in melting point with increased burnup. The relationship between melting point temperature and burnup shown in Fig. 8 was obtained experimentally by Christensen et al.[10]. The parameter T_m in Eq. (42) may be determined from Christensen's results. The melting point temperature of non-irradiated UO_2 was taken as 3073° by Christensen et al.

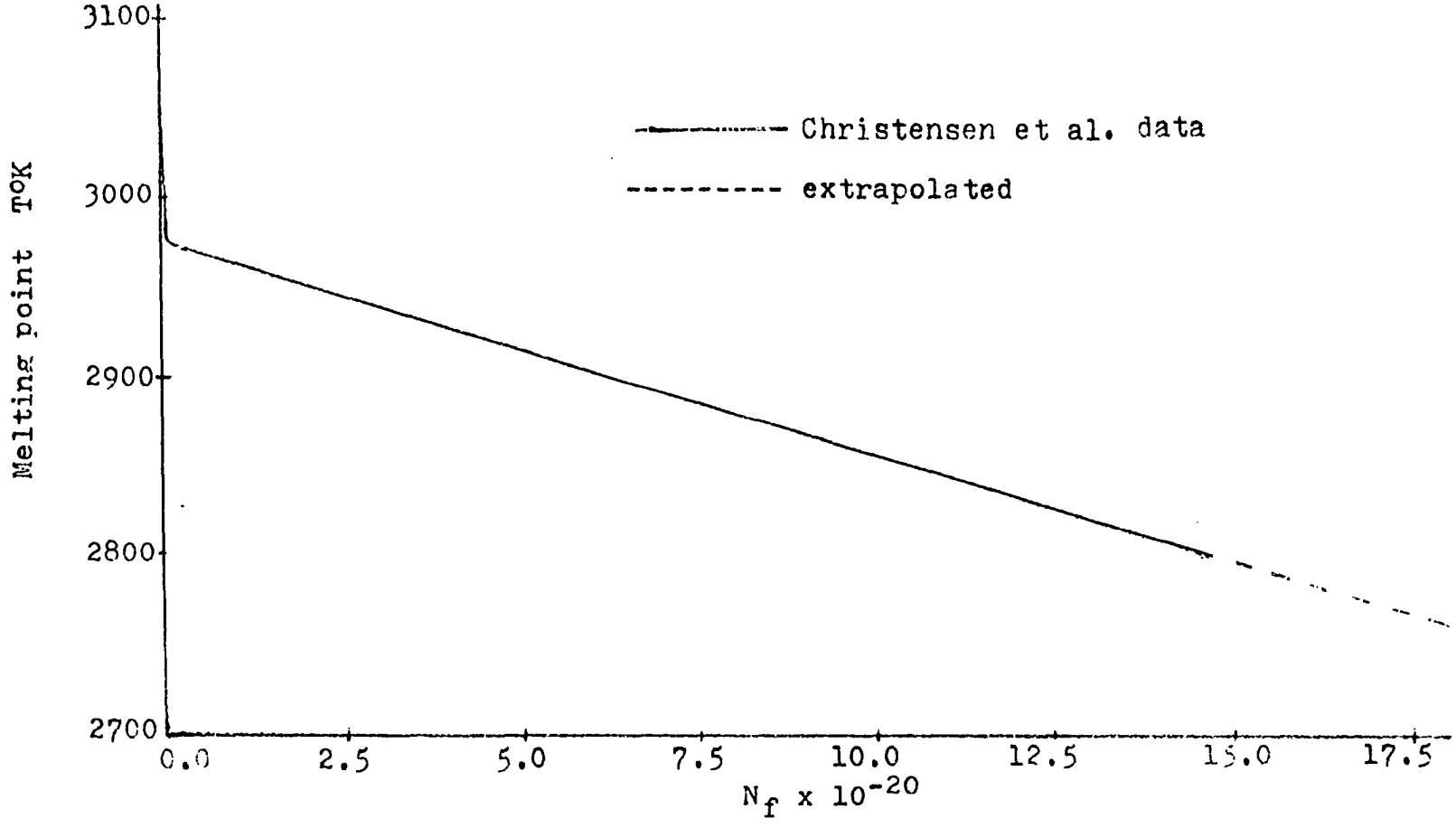

Fig. 8. Melting point of irradiated UO_2.

5. The mean mass $\bar{M}$

The mean mass of molecule in a partially used nuclear fuel should include fission products in its various burnup stages. The mean mass of the fission product will be based on the fission product yield data given by Frost [18] as shown in Table II.

About 25% of the fission products are gases. Among them 12% are noble gases such as xenon and krypton. It will be assumed here that all noble gases are lost from the fuel and all other gases are retained. For each UO_2 fission, two oxygen atoms would be left over. Some of these oxygen atoms may oxidize other fission products resulting in products such as MoO_3, SrO and BaO. About half of the oxygen atoms are assumed oxidized per fission and on the average, 1.5 oxygen atoms is assumed in excess and therefore no further oxidation occurs. From Frost's data, the mean mass of fission products is 67 grams per mole. From the fission product yeild data, it is estimated that approximately three impurities atoms and molecules were produced and retained in the fuel.

TABLE II

Fission Product Yield(EBR-II)[18]

Element	Fission product yield(atoms/100 fissions)			
	Oxide	Metal	Vapor	Total
Zr	26.9			26.9
Mo	12.8	10.3		23.1
Xe			22.3	22.3
Cs			19.0	19.0
Nd	17.6			17.6
Ru		16.9		16.9
Ce	13.8			13.8
Sr	7.4			7.4
Tc		0.1		0.1
Ba	6.1			6.1
La	6.0			6.0
Pr	5.0			5.0
Pd		4.8		4.8
Rh		4.2		4.2
Y	3.9			3.9
Sm	2.9			2.9
Pm	2.8			2.8
Te			2.7	2.7
Kr			2.5	2.5
I			1.3	1.3
Nb	1.0			1.0
Rb			0.6	0.6
Ag		0.5(liq)		0.5
Cd			0.4	0.4
Sn			0.3	0.3
Se			0.3	0.3
Eu	0.3			0.3
Sb			0.2	0.2
Br			0.1	0.1
Gd	0.1			0.1
Total				199.0

6. The parameter H

Eq. (42) may be used to determine the parameter H empirically. For a given burnup, K_L' is determined from the data of Asamoto et al. with density correction if it is necessary. The experimental data on irradiated UO_2 thermal conductivity K_L has not been explored extensively. However, a statistical values of irradiated UO_2 total thermal conductivity K basis on about a dozen experimental results under temperature of 1000°K have been shown by IAEA [22] and others [11]. Below 1000°K, the components K_e and K_r are assumed negligible and this will be proved to be so later. Therefore, IAEA's statistical values of K can be taken as approximately equal to K_L in Eq. (42) in order to determine the parameter H. It is found approximately that $H = 474 \pm 6$.

IV. CALCULATIONS AND RESULTS

To calculate the lattice component of thermal conductivity K_L from Eq. (42), it is first necessary to substitute Eq. (33) for K_L', $N_v = 1/\bar{V}$, $X = \sum_i x_i(M_i - \bar{M})^2$ and the values of

$$B = 0.0292$$

$$H = 474$$

$$M^{7/6}(UO_2) = 685$$

into Eq. (42). Then, re-arrange it into the form

$$K_L = (1.535 \times 10^{-15} \frac{T_m^2 \rho}{T} \frac{\bar{M}^{7/6}}{\bar{V}^{1/3} X})^{1/2} \cdot$$

$$\cdot \tan^{-1}(1.19 \times 10^6 \frac{T_m \rho^{1/3}}{T} \frac{\bar{V}^{1/3} X}{\bar{M}^{7/6}})^{1/2}$$

$$W/cm\text{-}^oK \qquad (45)$$

All of the parameters except the temperature T in Eq. (45) can be determined as a function of number of fissions per cm^3 N_f in the forms (see Appendix 1)

$$\bar{M} = \frac{3.294 \times 10^{24} - 34.5\, N_f}{1.22 \times 10^{22} + N_f}$$

$$\rho = 10.95 - 4.48 \times 10^{-22}\, N_f$$

$$X = \frac{(2.44 \times 10^{22} - N_f)(270 - \bar{M})^2 + 3N_f(67 - \bar{M})^2}{2.44 \times 10^{22} + 2N_f}$$

$$\bar{V} = \frac{1}{2.44 \times 10^{22} + 2N_f}$$

and T_m can be determined from Fig. 8 giving

$$T_m = 3070 - 12.5 \times 10^{-20} N_f$$

The electronic component of thermal conductivity K_e can be determined from Eq. (25) by assuming that the UO_2 above temperature $700^{\circ}K$ is an intrinsic semiconductor. After substituting the numerical values for K and e, it takes the form

$$K_e = 2.44 \times 10^{-8} \sigma T \qquad W/cm\text{-}^{\circ}K \qquad (46)$$

In determining the internal radiation component of thermal conductivity K_r, Eq. (27) will be used with the assumption that the refractive index n_r and absorption coefficient a_c are constant throughout all burnup stages. Substituting their numerical values and Stefan's constant given in Section III, K_r then has the form

$$K_r = 4.887 \times 10^{-13} T^3 \quad \text{W/cm-}^\circ\text{K} \qquad (47)$$

The total thermal conductivity K is to be determined at 7 temperature intervals from 700°K to 2500°K as a function of number of fissions/cm^3 N_f. As can be seen in Eq. (45) the component K_r is assumed to depend upon temperature only. Other components of dependence are both temperature and burnup. There will be 16 burnup intervals from 0.488×10^{20} fissions/cm^3 to 17.080×10^{20} fissions/cm^3, or 0.2% to 7.0% burnup.

A. The Lattice Component K_L

All parameters in Eq. (45) except temperature T are function of burnup. The functional relationship of K_L as a function of temperature T at various burnup has been calculated and shown in Table III, and the values of K_L at each temperature interval are shown in Table IV and Fig. 9.

TABLE III

Lattice Thermal Conductivity at Constant Burnup

$N_f \times 10^{-20}$	K_L
0.488	$3.53/T^{\frac{1}{2}} \tan^{-1}(10.0/T^{\frac{1}{2}})$
0.976	$2.34/T^{\frac{1}{2}} \tan^{-1}(15.2/T^{\frac{1}{2}})$
1.708	$1.90/T^{\frac{1}{2}} \tan^{-1}(18.6/T^{\frac{1}{2}})$
2.440	$1.62/T^{\frac{1}{2}} \tan^{-1}(21.8/T^{\frac{1}{2}})$
3.660	$1.26/T^{\frac{1}{2}} \tan^{-1}(26.5/T^{\frac{1}{2}})$
4.880	$1.09/T^{\frac{1}{2}} \tan^{-1}(31.4/T^{\frac{1}{2}})$
6.100	$1.01/T^{\frac{1}{2}} \tan^{-1}(33.6/T^{\frac{1}{2}})$
7.320	$0.92/T^{\frac{1}{2}} \tan^{-1}(36.3/T^{\frac{1}{2}})$
8.540	$0.86/T^{\frac{1}{2}} \tan^{-1}(38.5/T^{\frac{1}{2}})$
9.760	$0.80/T^{\frac{1}{2}} \tan^{-1}(41.5/T^{\frac{1}{2}})$
10.980	$0.75/T^{\frac{1}{2}} \tan^{-1}(43.5/T^{\frac{1}{2}})$
12.200	$0.71/T^{\frac{1}{2}} \tan^{-1}(45.5/T^{\frac{1}{2}})$
13.420	$0.68/T^{\frac{1}{2}} \tan^{-1}(46.9/T^{\frac{1}{2}})$
14.640	$0.65/T^{\frac{1}{2}} \tan^{-1}(48.3/T^{\frac{1}{2}})$
15.860	$0.63/T^{\frac{1}{2}} \tan^{-1}(49.5/T^{\frac{1}{2}})$
17.080	$0.60/T^{\frac{1}{2}} \tan^{-1}(51.0/T^{\frac{1}{2}})$

TABLE IV

Lattice Component of Thermal Conductivity

$N_f \times 10^{-20}$	K_L W/cm-°K						
	700°K	1000°K	1300°K	1600°K	1900°K	2200°K	2500°K
0.488	0.0480	0.0346	0.0263	0.0216	0.0183	0.0157	0.0145
0.976	0.0458	0.0334	0.0253	0.0211	0.0180	0.0152	0.0138
1.708	0.0435	0.0315	0.0243	0.0203	0.0173	0.0150	0.0135
2.440	0.0414	0.0302	0.0237	0.0198	0.0169	0.0146	0.0132
3.660	0.0380	0.0280	0.0223	0.0187	0.0160	0.0139	0.0125
4.880	0.0364	0.0268	0.0214	0.0182	0.0155	0.0135	0.0122
6.100	0.0344	0.0256	0.0206	0.0173	0.0149	0.0130	0.0117
7.320	0.0326	0.0246	0.0198	0.0169	0.0146	0.0127	0.0114
8.540	0.0310	0.0237	0.0190	0.0164	0.0142	0.0124	0.0112
9.760	0.0302	0.0225	0.0186	0.0160	0.0138	0.0123	0.0109
10.980	0.0288	0.0222	0.0180	0.0153	0.0134	0.0118	0.0107
12.200	0.0270	0.0216	0.0175	0.0148	0.0131	0.0115	0.0104
13.240	0.0267	0.0208	0.0168	0.0145	0.0128	0.0113	0.0102
14.640	0.0258	0.0203	0.0161	0.0142	0.0124	0.0110	0.0100
15.860	0.0253	0.0199	0.0158	0.0138	0.0122	0.0108	0.0098
17.080	0.0247	0.0192	0.0152	0.0134	0.0119	0.0106	0.0096

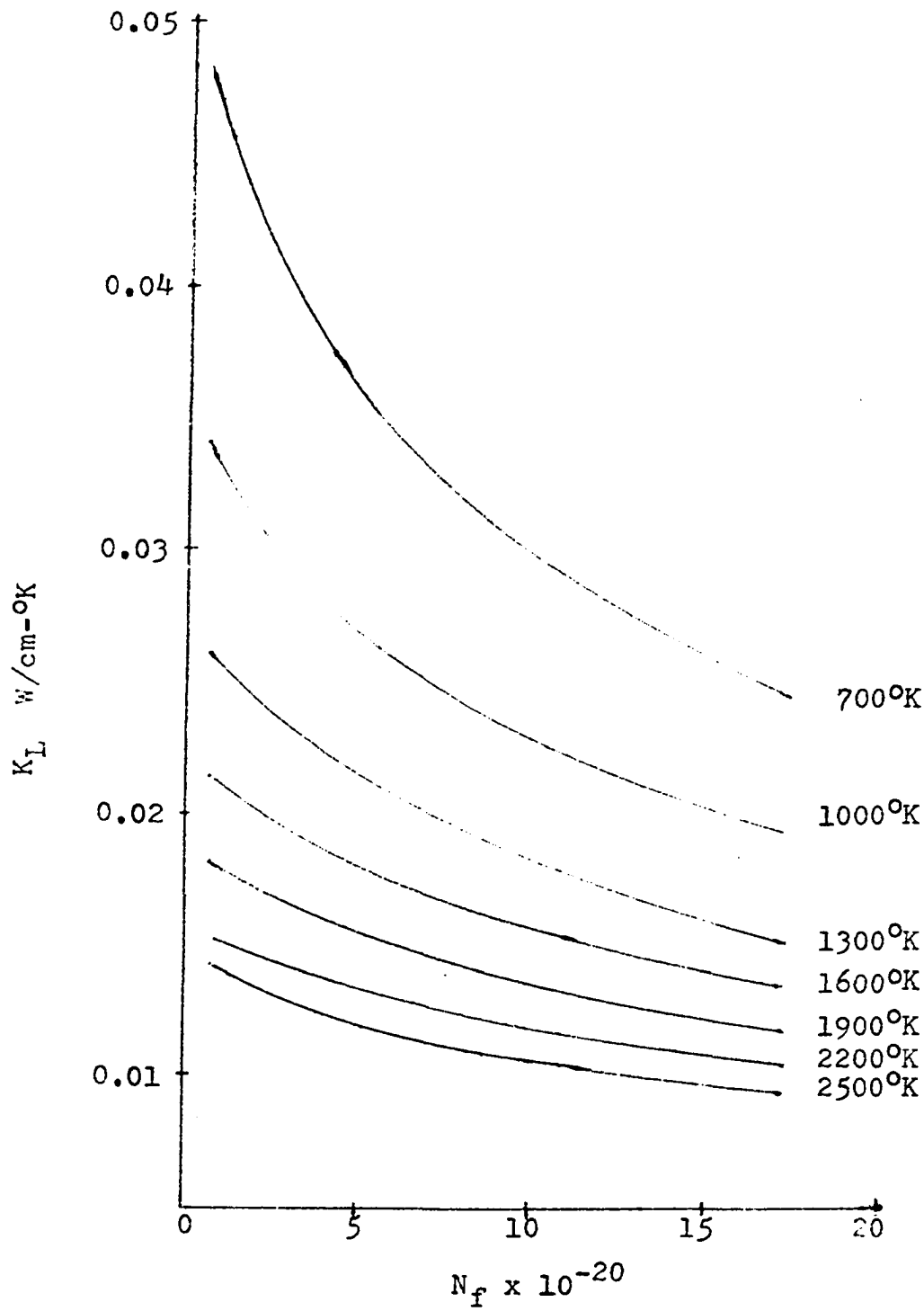

Fig. 9. Lattice component of thermal conductivity.

B. The Electronic Component K_e

In order to determine K_e by Eq. (46), the electrical conductivity σ at each burnup interval is first determined from Fig. 7, and the various values of electrical conductivity σ related to burnup and temperature are shown in Table V. Values of K_e are shown in Table VI. The values of x in Table VI refers to the non-stoichiometric UO_{2+x}.

C. Internal Radiation Component K_r

The internal radiation component of thermal conductivity depends upon temperature only. Its value at each temperature interval is calculated in Table VII and shown in Fig. 10.

D. The Total Thermal Conductivity K

The total thermal conductivity K is the sum of the values of K_L, K_e and K_r from Tables IV, VI and VII. The total thermal conductivity K at various conditions obtained are shown in Table VIII and plotted in Figs. 11 and 12.

TABLE V

Electrical Conductivity of Fission Depletion UO_2 Fuel

$N_f \times 10^{-20}$	x	σ (ohm-cm)$^{-1}$						
		700°K	1000°K	1300°K	1600°K	1900°K	2200°K	2500°K
0.488	0.006							
0.976	0.012							
1.708	0.021	0.05	0.26	0.47	0.68	0.86	1.06	1.26
2.440	0.030	0.10	0.36	0.58	0.81	1.04	1.28	1.50
3.660	0.046	0.20	0.52	0.85	1.18	1.50	1.83	2.17
4.880	0.061	0.22	0.67	1.08	1.50	1.91	2.34	2.75
6.100	0.077	0.28	0.81	1.27	1.84	2.35	2.88	3.38
7.320	0.092	0.35	1.00	1.60	2.19	2.79	3.38	3.98
8.540	0.109	0.40	1.13	1.83	2.52	3.23	3.93	4.13
9.760	0.125	0.43	1.27	2.07	2.86	3.68	4.47	5.77
10.980	0.141	0.50	1.43	2.34	3.22	4.12	5.00	5.92
12.200	0.158	0.55	1.60	2.60	3.59	4.60	5.58	6.58
13.240	0.172	0.60	1.75	2.87	3.95	5.06	6.15	7.26
14.640	0.191	0.65	1.94	3.18	4.40	5.60	6.80	8.02
15.860	0.208	0.70	2.10	3.40	4.70	6.00	7.30	8.55
17.080	0.226	0.75	2.25	3.65	5.05	6.64	7.87	9.35

TABLE VI

Electrical Component of Thermal Conductivity

$N_f \times 10^{-20}$	x	K_e W/cm-°K						
		700°K	1000°K	1300°K	1600°K	1900°K	2200°K	2500°K
0.488	0.006							
0.967	0.012							
1.708	0.021							
2.440	0.030							0.0001
3.660	0.046						0.0001	0.0001
4.880	0.061						0.0001	0.0002
6.100	0.077					0.0001	0.0002	0.0002
7.320	0.092					0.0001	0.0002	0.0002
8.540	0.109				0.0001	0.0002	0.0002	0.0003
9.760	0.125				0.0001	0.0002	0.0002	0.0004
10.980	0.141				0.0001	0.0002	0.0003	0.0004
12.200	0.158				0.0001	0.0002	0.0003	0.0004
13.240	0.172			0.0001	0.0002	0.0002	0.0003	0.0004
14.640	0.191			0.0001	0.0002	0.0003	0.0004	0.0005
15.860	0.208			0.0001	0.0002	0.0003	0.0004	0.0005
17.080	0.226			0.0001	0.0002	0.0003	0.0004	0.0006

TABLE VII

Internal Radiation Component of Thermal Conductivity

$T^{o}K$	K_r W/cm-^{o}K
700	0.0002
1000	0.0005
1300	0.0011
1600	0.0020
1900	0.0034
2200	0.0052
2500	0.0077

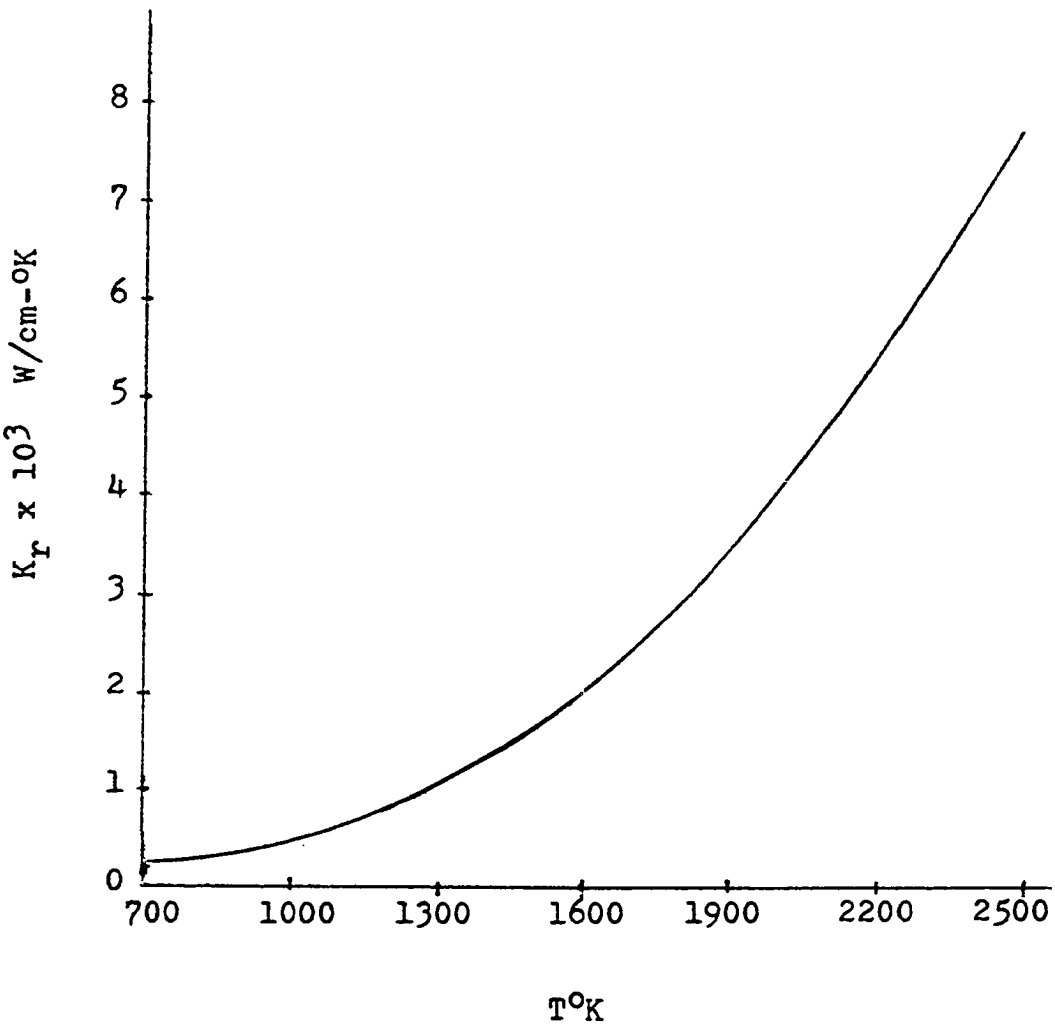

Fig. 10. Internal radiation component of thermal conductivity K_r.

TABLE VIII

Total Thermal Conductivity

K W/cm-°K

$N_f \times 10^{-20}$	700°K	1000°K	1300°K	1600°K	1900°K	2200°K	2500°K
0.488	0.0482	0.0351	0.0274	0.0236	0.0217	0.0209	0.0222
0.976	0.0460	0.0320	0.0265	0.0231	0.0214	0.0204	0.0215
1.708	0.0437	0.0307	0.0254	0.0223	0.0207	0.0202	0.0212
2.440	0.0416	0.0285	0.0244	0.0218	0.0203	0.0198	0.0209
3.660	0.0382	0.0282	0.0234	0.0207	0.0194	0.0192	0.0203
4.880	0.0366	0.0273	0.0225	0.0202	0.0189	0.0188	0.0201
6.100	0.0346	0.0261	0.0217	0.0193	0.0184	0.0184	0.0196
7.320	0.0328	0.0251	0.0209	0.0189	0.0181	0.0181	0.0193
8.540	0.0312	0.0242	0.0201	0.0185	0.0177	0.0178	0.0192
9.760	0.0304	0.0237	0.0197	0.0181	0.0174	0.0177	0.0189
10.980	0.0290	0.0227	0.0191	0.0174	0.0170	0.0172	0.0188
12.200	0.0272	0.0221	0.0186	0.0169	0.0167	0.0170	0.0185
13.240	0.0269	0.0213	0.0180	0.0167	0.0164	0.0168	0.0183
14.640	0.0260	0.0208	0.0173	0.0164	0.0161	0.0166	0.0182
15.860	0.0255	0.0204	0.0169	0.0160	0.0159	0.0164	0.0180
17.080	0.0249	0.0197	0.0164	0.0156	0.0156	0.0161	0.0179

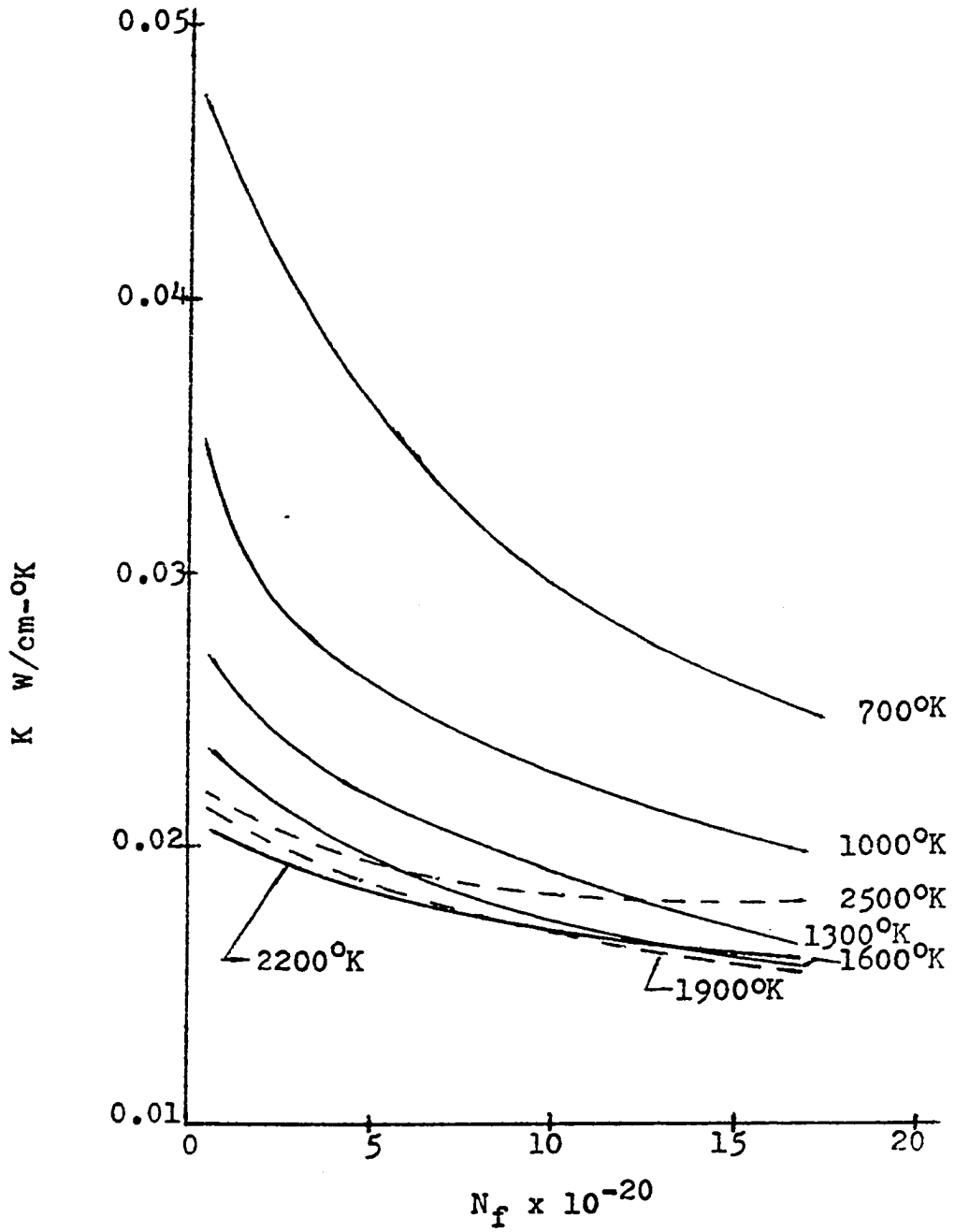

Fig. 11. Thermal conductivity K at constant temperature.

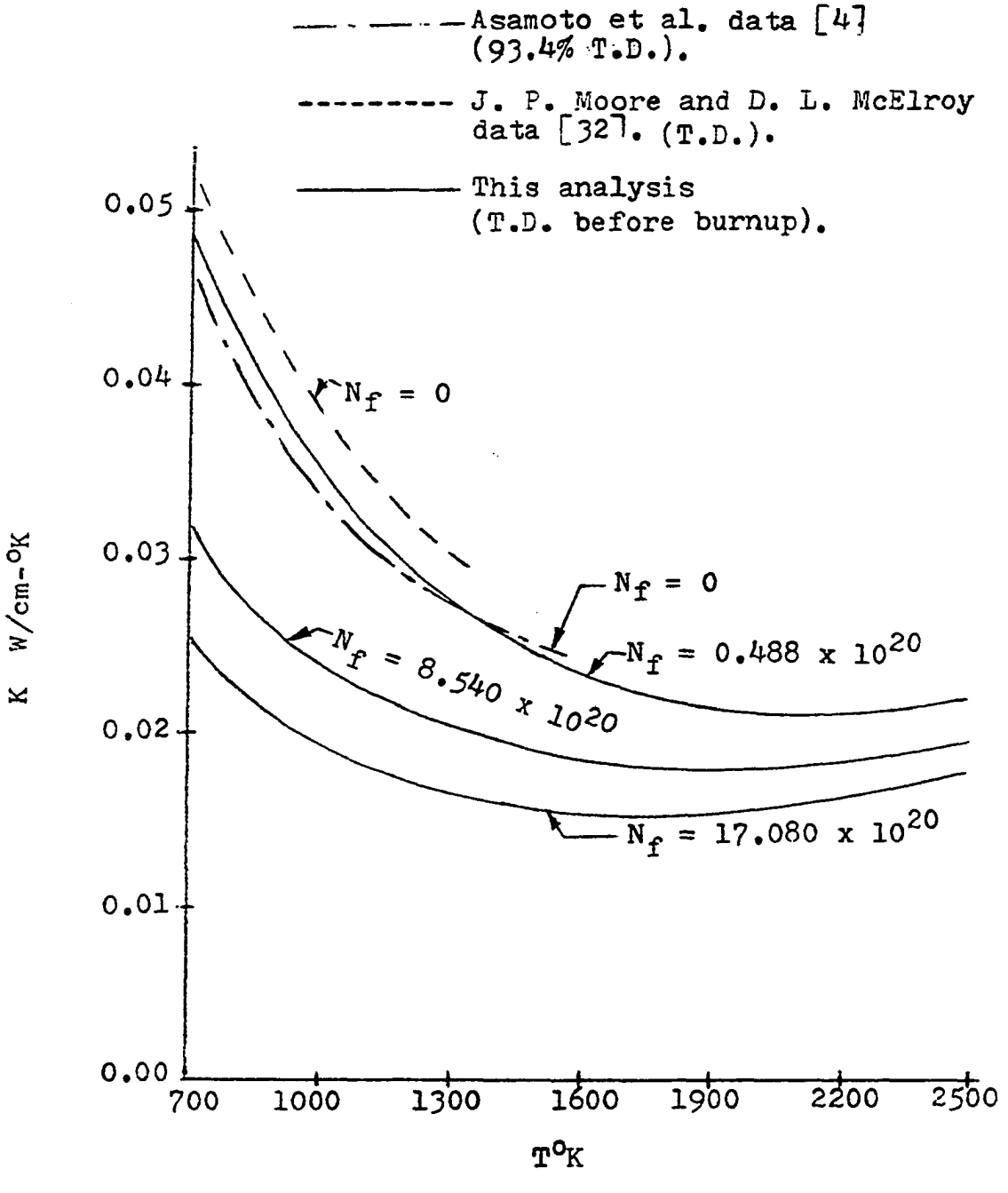

Fig. 12. Thermal conductivity K at constant burnup.

V. CONCLUSIONS AND DISCUSSIONS

From the results obtained in Section IV, the following conclusions may be derived.

1. The total thermal conductivity K is dominated by lattice component K_L. K_L is inversely proportional to both temperature and burnup, and the rate of K decrease become lower at higher temperatures and burnup.

2. The electron component K_e contributing to the total thermal conductivity K is insignificant. The most contribution by K_e to K is about 3.3% at temperature of 2500°K and burnup of 17.080×10^{20} fissions/cm^3. At lower temperature and burnup, K_e becomes negligible. This is because ceramic UO_2 is a poor electrical conductor.

3. Although small at low temperatures and burnups, the internal radiation component K_r contributing to total thermal conductivity K becomes very important at high temperatures and burnups. For example, at a temperature of 2500°K, K_r amounts to about 34% at a burnup of 0.488×10^{20} fissions/cm^3 and 43% at a burnup of 17.080×10^{20} fissions/

cm^3. This indicates that radiation is an important factor influencing the thermal conductivity of UO_2 nuclear fuel. Fortunately, this influence is positive.

4. The total thermal conductivity K at a given temperature is in general inversely proportional to burnup particularly at a relatively lower burnup range. At a given burnup, the total thermal conductivity K is a decreasing function of temperature in a relatively lower temperature range. At higher temperatures, due to the contribution of the internal radiation component K_r, K becomes directly proportional to temperature. The turning point temperature at which K changes from inverse function to a direct function of temperature depends upon the burnup. At a higher fuel burnups, the turning point temperature is relatively lower. This shows that internal radiation is more significant in a higher burnup fuel. This can be seen more clearly in Fig. 11, where the total thermal conductivity K at temperature 2500°K is higher than at temperatures 1900°K and 2200°K for all burnups. This is somehow unexpected.

From the forgoing conclusions and the results obtained above, it is evident that there is some temperature range at which the UO_2 fuel can achieve better performance as far as thermal conductivity is concerned. As shown in Fig. 11, the thermal conductivity K at temperature 2500°K is higher than at 1900°K and 2200°K at all burnup stages considered in this analysis. It is also higher than at temperatures of 1300°K and 1600°K for burnups above 12.5×10^{20} fissions/cm^3. Conclusively, a reactor operating at temperature 2500°K seems to be most attractive in terms of thermal conductivity. However, for a UO_2 fuel having a burnup of 17.08×10^{20} fissions/cm^3, the melting point temperature is about 2870°K, which is 370°K higher than the reactor operating temperature of 2500°K as mentioned above. This produces a margin of 370° or about 15% as far as temperature is concerned. Of course, at a lower burnup, the melting point temperature is higher. Hence, the temperature safety margin tends to increase.

The temperatures considered in this analysis are mean temperatures of the fuel. The thermal conductivity is therefore the mean thermal conductivity at that mean temperature. For a cylindrical geometry fuel, the temperature is higher in the region near the center. Thus, the thermal conductivity near the center line of the fuel where the tem-

perature is higher will be actually lower than the mean thermal conductivity as calculated. This must be kept in mind in order not to over estimate the thermal conductivity in a high temperature region above 1600°K which may lead to an unstable conditions.

It may be interesting although no effort will be made here to verify the internal radiation component of thermal conductivity K_r given by Eq. (47). Since the contribution of the electronic component of thermal conductivity K_e is small and may be neglected, then

$$K = K_L + K_r \tag{48}$$

As can be seen in Table IV, the product of $K_L T$ is fairly constant at a given fuel burnup, and K_L is a function of temperature only. At low temperature, K_r is small and $K \approx K_L$, hence KT is a constant. As the temperature rises, K_r becomes significant and hence KT would no longer be constant but also increases. Let T_1 represent a relatively lower temperature where K_r is negligible and T_2 represent a higher temperature where K_r becomes significant. Then K_r may be expressed as

$$K_{r2}T_2 = K_2T_2 - K_1T_1$$

hence

$$K_{r2} = \frac{K_2T_2 - K_1T_1}{T_2} \qquad (49)$$

where K_{r2} is K_r at temperature T_2. K_1 and K_2 are the total thermal conductivity K at temperatures T_1 and T_2 respectively. This method may be used to determine either the refractive index n_r or absorption coefficient a_c if the other is known.

The most distinctive feature of this analysis is its application of Lindemann's melting rule to form a theoretical basis for developing the semi-empirical Eq. (45) that can be used to determine the thermal conductivity of UO_2 nuclear fuel with continuously changing physical properties as a result of its increased burnup. The advantages of Eq. (45) are as follows: 1. It has two independent variables namely: temperature T and number of fissions per cm^3 N_f. Thus, the thermal conductivity can be determined for any given T and N_f if temperature is not higher than the melting point temperature and N_f is within the practical reactor burnup range. 2. It offers a unique method of dealing with the UO_2 fuel thermal conductivity problem not only quantitatively but also qualitatively. 3. The same

method employed in this analysis can be also used to determine thermal conductivities of other nuclear fuels such as PuO_2.

Numerous assumptions have been made in deriving the lattice component of thermal conductivity K_L both in the literatures cited and by this author. Although those assumptions were considered highly reasonable, the possibility of some over simplification may exist. However, the empirical factors B and H introduced on the basis of experimental data are to correct such possibilities.

The parameters T_m, ρ, $\bar{V}$, $\bar{M}$ and X in Eq. (45) are all functions of number of fissions/cm^3 N_f as derived in Appendix 1. Therefore, it is possible to write Eq. (45) as a function of the two independent variables T and N_f only. However, Eq. (45) will be retained because it is relatively convenient in performing calculations and showing more details of its physical contents.

Eq. (45) is not applicable to non-irradiated fuel, because in a non-irradiated fuel, $M_i = \bar{M}$, hence $X = 0$ where the function is discontinuous.

One of the purpose of this analysis is to determine the in-pile conditions of thermal conductivity of UO_2 during neutron irradiation. However, as has been shown in Section III, the migration of fission gases and the ionization of fission fragments which occur during irradiation make a negligible contribution to energy transport processes. Therefore, it can be concluded that the difference in thermal conductivity between in-pile and out-of-pile measurements is negligible.

VI. SUGGESTION FOR FUTURE STUDY

The disagreements among various experimental results may arise from many sources. One of the sources may come from the fission rate and frequency of changing fission rates. Out-of-pile experimental measurements can be made to verify this.

Three identical samples may be provided, two of them irradiated at different but constant reactor power levels, a third irradiated with various reactor power levels until all three of them have attained the same total fission depletion before each sample is taken out of the reactor. The cooling time of these three samples must be the same when the thermal conductivity measurements are performed.

If there are any differences in thermal conductivities among these samples, a knowledge of thermal conductivity related to irradiation histories may be gained. This will be an advantage to the UO_2 fuel designers.

VII. LITERATURE CITED

1. J. B. AINSCOUGH and M. J. WHEELER, Brit. J. Appl. Phys. (J. Phys. D), 1, 859 (1968).
2. V. AMBEGAOKAR, Phys. Rev., 114, 488 (1959).
3. A. J. ANGSTROM, J. Ann. Physik., 114, 531 (1861).
4. R. R. ASAMOTO, F. L. ANSELIN and A. E. CONTI, J. Nucl. Mater., 29, 67 (1969).
5. J. L. BATES, " Fission Fragment and Plutonium Distribution in UO_2," HW-81601, General Electric (1964).
6. J. L. BATES, Trans. Am. Nucl. Soc., 7, 389 (1964).
7. J. L. BATES, C. A. HINMAN and T. KAWADA, J. Am. Ceram. Soc., 50, 652 (1967).
8. M. BOGAIEVSKI, R. CALLIAT, R. DELMAS, J. C. JANVIER and J. A. L. ROBERTSON, in Conf. on New Nucl. Mater. Including Non-metallic Fuel, Vol. 1, p. 307, IAEA, Vienna (1963).
9. T. B. BURLEY and M. D. FRESHLEY, Nucl. Appl. and Tech., 9, 233 (1970).
10. J. A. CHRISTENSEN, R. J. ALLIO and A. BIANCHERIA, Trans. Am. Nucl. Soc., 7, 390 (1964).
11. R. C. DANIEL and I. COHEN, "In-pile Effective Thermal Conductivity of Oxide Fuel Elements to High Fission Depletion," WAPD-246, Westinghouse Electric Corp. (1964).

12. G. C. DANIELSON and P. H. SIDLE, in Thermal Conductivity, Vol. 2, R. P. Tye, Ed., p. 149, Academic Press, New York (1969).

13. P. DEBYE, Vorträge über die Kinetische Theorie, (1914). Original not available; cited in R. W. KEYES, Phys. Rev., 115, 564 (1959).

14. D. R. DE HALAS, Nucleonics, 21, 92 (1963).

15. C. C. DOLLINS and H. OCKEN, Nucl. Appl. and Tech., 9, 141 (1970).

16. J. R. DRABBLE and H. J. GOLDSMID, Thermal Conduction in Semiconductors, pp. 33-164, Pergamon Press, New York (1961).

17. J. S. DUGDALE and K. C. MACDONALD, Phys. Rev., 98, 1751 (1955).

18. B. R. T. FROST, Nucl. Appl. and Tech., 9, 128 (1970).

19. L. GENZEL, Z. Phys., 135, 177 (1953).

20. T. G. GODFREY, W. FULKERSON, T. G. KOLLIE, J. P. MOORE and D. L. MCELROY, J. Am. Ceram. Soc., 48, 297 (1965).

21. H. J. GOLDSMID, Proc. Phys. Soc. London, B69, 203 (1956).

22. IAEA, "Thermal Conductivity of Uranium Dioxide," Tech. Reports Ser. No. 59, IAEA, Vienna (1966).

23. A. V. IOFFE and A. F. IOFFE, Zh. Tekh., 22, 2005 (1952).

24. T. ISHII, K. KEIJI and K. OSHIMA, J. Nucl. Mater., 36, 288 (1970).

25. R. W. KEYES, Phys. Rev., 115, 564 (1959).

26. C. KITTEL, Intro. to Solid State Physics, 2 ed., p. 142, John Wiley & Son, Inc., New York (1953).

27. P. G. KLEMENS, Phys. Rev., 119, 507 (1960).

28. P. G. KLEMENS, in Thermal Conductivity, Vol. 1, R. P. Tye, Ed., p. 2, Academic Press, New York (1969).

29. M. J. LAUBITZ, in Thermal Conductivity, Vol. 1, R. P. Tye, Ed., p. 111, Academic Press, New York (1969).

30. A. W. LAWSON, J. Phys. Chem. Solid, 3, 155 (1957).

31. F. A. LINDEMANN, Phys. Z., 11, 609 (1910).

32. D. L. MCELROY and J. P. MOORE, in Thermal Conductivity, Vol. 1, R. P. Tye, Ed., p. 186, Academic Press, New York (1969).

33. J. P. MOORE and D. L. MCELROY, J. Am. Ceram. Soc., 54, 40 (1971).

34. G. J. MORGAN, J. Phys. C (Proc. Phys. Soc.), 1, 347 (1968).

35. A. M. ROSS, "The Dependence of the Thermal Conductivity of Uranium Dioxide on Density, Microstructure, Stoichiometry and Thermal-neutron Irradiation," CRFD-817, Atomic Energy of Canada Limited (1960).

36. W. SHOCKLEY, Electrons and Holes in Semiconductors, pp. 12-15, D. Van Nostrand Company, Inc., New York (1950).

37. R. VISKANTA, Nucl. Sci. Eng., 21, 12 (1965).

38. R. K. WILLARDSON, J. W. MOODY and H. L. GOERING, J. Inorg. Nucl. Chem., 6, 19 (1958).

39. R. K. WILLARDSON and J. W. MOODY, in Uranium Dioxide: Properties and Nuclear Applications, J. Belle, Ed., p. 217, Naval Reactors, Division of Reactor Development, USAEC (1961).

40. J. M. ZIMAN, Electrons and Phonons, pp. 218-420, Oxford University Press, London (1960).

VIII. ACKNOWLEDGEMENTS

The author wishes to express his sincere gratitude to Dr. Glenn Murphy for his advice and guidance throughout the development of this dissertation.

Thanks are also due to the author's wife for her understanding during the last few years.

IX. APPENDIX: DERIVATION OF PARAMETERS

A. The Mean Mass $\bar{M}$

The mean mass $\bar{M}$ is defined as

$$\bar{M} = \sum_i x_i M_i \qquad (A.1)$$

where x_i is the fraction of ith molecular of mass M_i per mole. The mass per mole of fission products has been determined from Table II and it is assumed in Section III that the mean mass per mole of fission products is 67 grams. The mass per mole of UO_2 is approximately 270 grams. From these assumptions, the molecules may be roughly grouped into two groups, namely: the UO_2 and fission products, so Eq. (A.1) can be written

$$\bar{M} = x_u M_u + x_f M_f \qquad (A.2)$$

where the subscripts u and f are UO_2 and fission products respectively. Let N_{TD} and N_f denote the number of UO_2 molecules per cm^3 at theoretical density and the number of fissions per cm^3 respectively. Therefore, x_u and x_f can be given in the form

$$x_u = \frac{N_{TD} - N_f}{(N_{TD} - N_f) + 3N_f} = \frac{N_{TD} - N_f}{N_{TD} + 2N_f} \qquad (A.3)$$

where $3N_f$ in the above equation is a result of 3 fission products, one light nucleus, one heavy nucleus and one oxygen approximately having been produced from one UO_2 fissioned.

$$x_f = \frac{3N_f}{N_{TD} + 2N_f} \qquad (A.4)$$

Hence

$$\bar{M} = \frac{(N_{TD} - N_f)M_u + 3N_fM_f}{N_{TD} + 2N_f}$$

$$= \frac{N_{TD}M_u - (M_u - 3M_f)N_f}{N_{TD} + 2N_f} \qquad (A.5)$$

with $M_u = 270$, $M_f = 67$ and $N_{TD} = 10.95$ grams/cm^3 determined from theoretical density, gives

$$\bar{M} = \frac{3.294 \times 10^{24} - 34.5N_f}{1.22 \times 10^{22} + N_f} \qquad (A.6)$$

B. The Mean Volume Per Molecule $\bar{V}$

The mean volume per molecule is defined as

$$\bar{V} = 1/N_v \tag{A.7}$$

where N_v is number of molecules per unit volume, that is

$$N_v = (N_{TD} - N_f) + 3N_f$$

$$= N_{TD} + 2N_f \tag{A.8}$$

hence

$$\bar{V} = \frac{1}{2.44 \times 10^{22} + 2N_f} \tag{A.9}$$

C. The Density ρ

The density ρ of UO_2 at any fuel burnup interval is

$$\rho = \rho_{TD} - \rho_f \tag{A.10}$$

where ρ_f is the density of fissioned portion of UO_2, and not density of fission products. It can be given by

$$\rho_f = \frac{M_u}{N_a} N_f = 4.48 \times 10^{-22} N_f \tag{A.11}$$

where N_a is Avogadro's number. With $\rho_{TD} = 10.95$ gm/cm^3,

$$\rho = 10.95 - 4.48 \times 10^{-22} N_f \qquad (A.12)$$

D. The Parameter X

The parameter X is defined as

$$X = \sum_i x_i (M_i - \bar{M})^2 \qquad (A.13)$$

where x_i, M_i and $\bar{M}$ were defined in Appendix A, then X can be written in the form

$$X = \frac{(N_{TD} - N_f)(270 - \bar{M})^2 + 3N_f(67 - \bar{M})^2}{2.44 \times 10^{22} + 2N_f} \qquad (A.14)$$

Substituting the numerical value for N_{TD}, X becomes

$$X = \frac{(2.44 \times 10^{22} - N_f)(270 - \bar{M})^2 + 3N_f(67 - \bar{M})^2}{2.44 \times 10^{22} + 2N_f} \qquad (A.15)$$

where $\bar{M}$ is determined by Eq. (A.5).